Electronic Transactions on Numerical Analysis.
Volume 8, pp. 46-87, 1999.

ISSN 1068-9613.

ETNA
Kent State University
etna@mcs.kent.edu

ON THE CONVERGENCE OF MULTIGRID METHODS FOR FLOW PROBLEMS*

INGEMAR PERSSON†, KLAS SAMUELSSON‡, AND ANDERS SZEPESSY§

Abstract. We prove two theorems on the residual damping in multigrid methods when solving convection dominated diffusion equations and shock wave problems, discretized by the streamline diffusion finite element method. The first theorem shows that a V-cycle, including sufficiently many pre and post smoothing steps, damps the residual in L_1^{loc} for a constant coefficient convection problem with small diffusion in two space dimensions, without the assumption that the coarse grid is sufficiently fine. The proof is based on discrete Green's functions for the smoothing and correction operators on a uniform unbounded mesh aligned with the characteristic. The second theorem proves a similar result for a certain continuous version of a two grid method, with isotropic artificial diffusion, applied to a two dimensional Burgers shock wave problem. We also present numerical experiments that verify the residual damping dependence on the equation, the choice of artificial diffusion and the number of smoothing steps. In particular numerical experiments show improved convergence of the multigrid method, with damped Jacobi smoothing steps, for the compressible Navier-Stokes equations in two space dimensions by using the theoretically suggested exponential increase of the number of smoothing steps on coarser meshes, as compared to the same amount of work with constant number of smoothing steps on each level.

Key words. multigrid methods, convergence, convection-diffusion, conservation laws, Green's function, shock waves.

AMS subject classifications. 65N55, 65N30, 35L65.

1. Introduction. In this paper, we analyze multigrid algorithms for solving discrete equations approximating stationary convection dominated diffusion equations and a shock wave problem in a scalar conservation law in two space dimensions. We focus our theoretical analysis on model problems and compare with numerical experiments, including more general problems as the compressible Navier-Stokes equations. A conclusion from our analysis and experiments, for a multigrid method with damped Jacobi smoothing steps, is that it is advantageous to increase the number of smoothing steps on coarser levels, as compared to the same amount of work with constant number of smoothing steps on each level.

We first consider the convection-diffusion problem to find u such that

$$\begin{aligned} &xu_{x_1} - \epsilon\Delta u = F, \quad x = (x_1, x_2) \in \Omega \subseteq \mathbb{R}^2, \\ &xu|_{\partial\Omega} = 0, \end{aligned} \tag{1.1}$$

where F is a given source function and $\epsilon > 0$ is a given small constant. We shall study multigrid algorithms for solving, approximately, the streamline-diffusion finite element equations, cf. [19], of (1.1): Find $U \in V_h$, such that

$$a_h(U, v) \equiv (U_{x_1}, v + \frac{h}{2}v_{x_1}) + (\epsilon\nabla U, \nabla v) = (F, v + \frac{h}{2}v_{x_1}) \quad \forall v \in V_h, \tag{1.2}$$

where V_h is a usual finite element space of continuous functions that are linear (i.e. they belong to $\mathcal{P}_1(K)$) on each triangle K in a mesh T^h of Ω, with mesh size h,

$$V_h \equiv \{v \in H_0^1(\Omega) : v|_K \in \mathcal{P}_1(K)\ \forall K \in T^h\}$$

*Received July 25, 1997. Accepted January 12, 1999. Recommended by T. Chan. This work was supported by TFR grant 92691 and TMR project HCL ERBFMRXCT960033.

†Institutionen för Numerisk Analys och Datalogi, Kungl. Tekniska Högskolan, S-100 44 Stockholm. (ipe@nada.kth.se)

‡Matematiska Institutionen, Chalmers Tekniska Högskola, S-412 96 Göteborg. (klassam@math.chalmers.se)

§Institutionen för Numerisk Analys och Datalogi, Kungl. Tekniska Högskolan, S-100 44 Stockholm. (szepessy@nada.kth.se)

ETNA
Kent State University
etna@mcs.kent.edu

and

$$(v, w) \equiv \int_\Omega v(x)w(x)dx.$$

Here $H_0^1(\Omega)$ denotes the Sobolev space of functions that vanish on $\partial\Omega$ and have one derivative in $L_2(\Omega)$. The multigrid algorithm is based on a hierarchy of refined meshes with corresponding finite element spaces $V_j \equiv V_{h_j}$, with the sets of nodal points $\mathcal{N}_j = \{x_i\}_{i=1}^{N_j}$, $j = 0, 1, 2, \ldots J$, where $V_0 \supset V_1 \supset V_2 \ldots \supset V_J$. Starting with an approximate solution $U_0 \in V_0 = V_h$ of U in (1.2), the first step in the multigrid method is the smoothing operation $S_{0,F} : V_0 \to V_0$ defined by the damped Jacobi method with a suitable small positive damping constant c, (pre) smoothing steps $m = 0, 1, \ldots, \nu_0 - 1$ and

$$\begin{array}{ll} & \bar{U}_0 = U_0, \\ (1.3) & \bar{U}_{m+1}(x_i) = \bar{U}_m(x_i) - \frac{c}{h_0}[a_0(\bar{U}_m, \phi_i) - (F, \phi_i + \frac{h_0}{2}\phi_{i,x_1})] \quad \forall x_i \in \mathcal{N}_j, \\ & S_{0,F}\bar{U}_0 \equiv \bar{U}_{\nu_0}. \end{array}$$

Here, for $j = 0, 1, 2, \ldots, J$, we use that $a_j(\cdot, \cdot) \equiv a_{h_j}(\cdot, \cdot)$, h_j is the mesh size in V_j, and $\mathcal{B}_j \equiv \{\phi_i\}_{i=1}^{N_j}$ is the standard basis in V_j, i.e. $\phi_i \in V_j$ together with

$$(1.4) \qquad \phi_i(x_k) = \begin{cases} 1, & k = i, \\ 0, & k \neq i, \end{cases}$$

for all i and nodal points $x_k \in \mathcal{N}_j$. The basis (1.4) implies the representation

$$(1.5) \qquad \bar{U}_m(x) = \sum_{i=1}^{N_j} \bar{U}_m(x_i)\phi_i(x), \quad \text{for } \bar{U}_m \in V_j.$$

Consider the special case of $J = 1$, i.e. the two grid method, and an approximation $U_0 \in V_0$ of U in (1.2). Then, the first approximation $\bar{U}_{\text{next}}^{\text{pre}} \in V_0$ is

$$(1.6a) \qquad \bar{U}_{\text{next}}^{\text{pre}} = S_{0,F}U_0 - d,$$

where the coarse grid correction $d \in V_1$ on the finest level is defined by

$$(1.6b) \qquad a_1(d, v) = a_0(S_{0,F}U_0, v) - (F, v + \frac{h_0}{2}v_{x_1}) \quad \forall v \in V_1.$$

By including also post smoothing, the next approximation is

$$(1.7) \qquad \bar{U}_{\text{next}} = S_{0,F}\bar{U}_{\text{next}}^{\text{pre}}.$$

Assumption 1.8. In a multigrid V-cycle iteration, the correction equation (1.6b) on $V_j = V_1$ is solved approximately by recursivly applying smoothing steps, on level j, and its correction in V_{j+1}. The correction equation on V_J is solved exactly. We analyze the convergence of this V-cycle iteration with pre and post smoothing by studying an approximation U_0 of U and its next iterate U_{next}, which is the multigrid approximation of the two grid solution $\bar{U}_{\text{next}}$ in (1.7).

We use a multigrid method applicable to elliptic problems as well as to shock wave problems described by conservation laws, and focus on the analysis of a special and simple but general applicable multigrid method. Therefore, we study the damped Jacobi smoothing operator which is independent of the ordering of the nodes, although, for the problem (1.1),

ETNA
Kent State University
etna@mcs.kent.edu

the convergence can be improved by ordering the nodes in the direction of the flow and for applying Gauss-Seidel iterations in the smoothing steps; see [8] and related results for domain decomposition methods [11], [23]. The one dimensional problem corresponding to (1.1) and (1.2) with x_2 the independent solution, and $\epsilon = 0$, yields a bilinear form a which reduce to the upwind operator. Therefore, smoothing steps based on an ordering of the nodes in the x_1 direction can solve this one dimensional problem (1.2) in one step. However, for flows in two and three dimensions, which do not have typical inflow and outflow regions, ordering of the nodes is hard to achieve.

In this work we present two theorems on the residual damping in multigrid methods solving convection dominated diffusion equations and shock wave problems, discretized by the streamline diffusion finite element method. Usually, the convergence study of multigrid methods for elliptic problems uses the iteration error and its behavior in energy norms. Our study focuses on the residual and its L_1-norm, and the analysis is based on Green's functions, which motivate the use of L_1-norms. Theorem 1.1, below, proves that a V-cycle, including sufficiently many pre and post smoothing steps, damps in L_1 a residual, initially localized inside Ω, for a constant coefficient convection problem with small diffusion in two space dimensions, without the assumption that the coarse grid is sufficiently fine. The proof is based on discrete Green's functions related to the smoothing and correction operators.

Theorem 1.2, below, proves a similar result for a certain continuous version of a two grid method, with isotropic artificial diffusion, applied to a two dimensional Burgers shock wave problem. We compare, in Fig. 1 and Section 7, the result of Theorems 1.1 and 1.2 with numerical experiments describing the residual damping dependence on the equation, the choice of artificial diffusion and the number of smoothing steps.

To have an efficient multigrid method, V-cycles must reduce and damp the residual. The numerical test in Fig. 1, below, shows the residual damping of one V-cycle applied to (1.1). In the Experiments I and II, initially the L_1-norm of the residual is equal to 1 and localized to a point in the center of the domain. The L_1-norm $\gamma(n)$ of the residual after n V-cycles, $n = 1$ and $n = 5$, in Experiments I and II respectively, are computed as the number of pre and post smoothing steps are increased. Experiment II shows the asymptotic average damping $\bar{\gamma} \equiv (\gamma(5)/\gamma(1))^{1/4}$ of a V-cycle in the multigrid method with many cycles. We see that the damping from an initially localized residual is similar to the (generic) one of Experiment III in Fig. 1. Moreover, we note that the damping $\gamma(1)$ can be made smaller by increasing ν. How does $\gamma(1)$ depend on ν, ϵ and J? How many smoothing steps should we take on each level to obtain optimal damping? Theorem 1.1, below, answers these questions of $\gamma(1)$. In Section 7.2, we discuss the effect of several V-cycles on the average damping. Further numerical results on elliptic, convection and shock wave problems are given in Sections 7 and 8.

The first theorem on residual daming avoids possible boundary effects by assuming that the residual $R(v) \equiv a_0(U_0, v) - (F, v + hv_{x_1}/2)$ is supported inside Ω, *i.e.* $R(v) = 0$ for all v supported in a neighborhood of $\partial\Omega$. To further simplify the analysis we assume that $u(x) \to 0$, as $|x| \to \infty$, and that $\Omega = I\!R^2$ is discretized by a uniform mesh where the characteristic direction $(1, 0)$ is aligned with the mesh. Our analysis of the damping requires precise information of the residuals evolution in the V-cycle. The requirement for extensive information restricts us to model cases, which we, on the other hand, can describe in detail. For instance, it is shown in Section 7.1 that the the residual damping depends on the orientation of the mesh with respect to the characteristics. In Section 2, we derive an error representation for the multigrid V-cycle iterations based on the smoothing and correction steps for the problem (1.1). In Section 3, we first formulate an evolutionary Green's function problem and derive its representation of V-cycle iteration errors, and then we give an overview

ETNA
Kent State University
etna@mcs.kent.edu

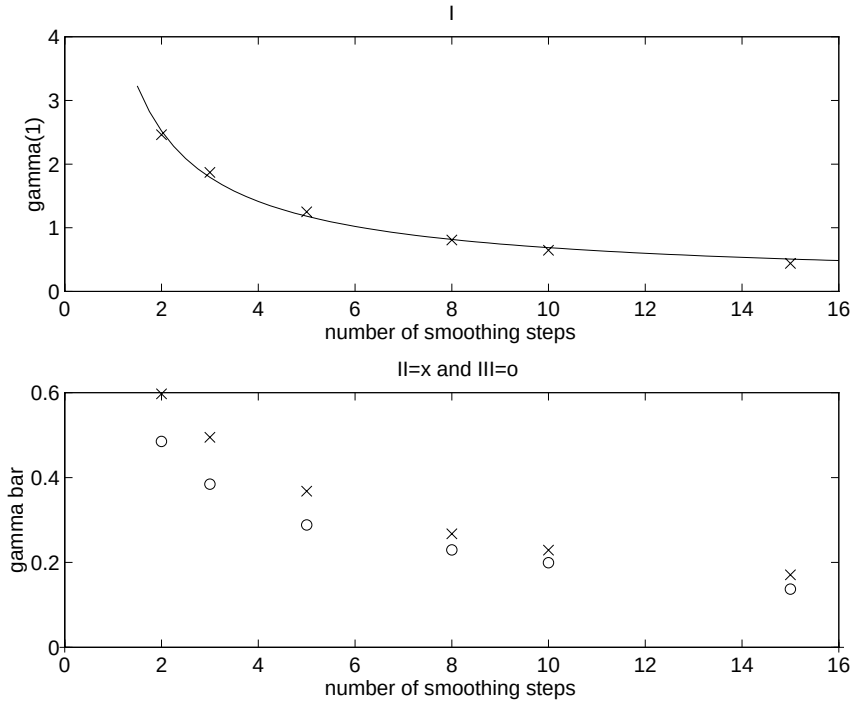

FIG. 1. *Residual damping rate of multigrid V-cycles. We use multigrid iterations to solve (1.1) in the computational domain* $\Omega = (0,1) \times (0,1)$*, with* $\epsilon = h_0$ *and homogeneous Dirichlet boundary conditions. For a description of the parameters used in the multigrid cycle see Table 1, Experiment A in Section 7. Experiments* I *(upper figure* $\times$*) and* II *(lower figure* $\times$*) start with an initial Dirac-like algebraic residual with* L_1*-norm equal to 1.0 at the center of the computational domain. Experiment* I *depicts the* L_1*-norm* $\gamma(n)$ *of the residual after one V-cycle (i.e.* $n = 1$*) as a function of the number of smoothing steps* ν*. The solid line in the upper figure is given by* $\hat{C}_1/\nu + \hat{C}_2\sqrt{\nu}$*, cf. (1.10), where* $\hat{C}_1 = 3.56, \hat{C}_2 = 1.05$ *are determined as the least square fit to the data* $\times$*. The asymptotic damping is defined to be the average reduction factor* $\bar{\gamma} \equiv (\gamma(m)/(\gamma(1))^{1/(m-1)}$*,* $m \to \infty$*, of the* L_1*-norm of the residual in two consecutive V-cycles. Experiments* II *and* III *depict asymptotic damping factors where we have chosen* $m = 5$*, for two different initial residuals. In Experiment* II *the initial residual is a Dirac-delta function. The third Experiment* III*, denoted by* o*, depicts the asymptotic damping of the multigrid method applied to (1.1), with an initial guess* $U_0 = 0$ *and* $F = \sin(10x)\sin(15y)$*. Theorems 1.1 and 1.2 treat* $\gamma(1)$*, and Section 7.2 studies* $\gamma(n),\ n > 1$*.*

of the proof of residual damping stated in Theorem 1.1. This overview is an attempt to explain the idea of the proof on one page. The full proof in Sections 4-6 is basically an extension of the overview, which is based on differential operators, to discrete difference operators. The proof uses Fourier methods to analyze the evolutionary Green's function problem on a uniform mesh. Our main result is

THEOREM 1.1. *Let* $\Omega = \mathbb{R}^2$ *be discretized by a hierarchy of uniform meshes, with triangle edges in the direction* $(1,0), (0,1)$ *and* $(1,1)$*, where the mesh size,* h_j*, on level* j*,*

ETNA
Kent State University
etna@mcs.kent.edu

satisfies

$$h_j = 2h_{j-1}, \quad j = 1, 2, \ldots, J,$$

and, on the finest level, $j = 0$*,*

$$h_0 \geq 3\epsilon.$$

Define the set

$$V_\beta^1 \equiv \{v \in V_0 : \|v\|_{L_\infty} \leq 1,\ v(x_1, \cdot) = 0 \text{ for } |x_1| > \beta\},$$

and assume that, for some $B > 0$*, the residual error is supported in* $[-B, B] \times I\!R$*, i.e.*

$$a_0(U_0, v) - (F, v + \frac{h_0}{2} v_{x_1}) = 0 \quad \forall v \in \{w \in V_0 : w(x_1, \cdot) = 0 \text{ for } |x_1| \leq B\}.$$

Then the quotient of residuals, measured in $L_1([-B, B] \times I\!R)$*,*

$$\gamma_B \equiv \frac{\sup_{v \in V_B^1} |a_0(U_{\text{next}}, v) - (F, v + \frac{h_0}{2} v_{x_1})|}{\sup_{v \in V_\infty^1} |a_0(U_0, v) - (F, v + \frac{h_0}{2} v_{x_1})|}, \tag{1.9}$$

for two consecutive V-cycle iterates U_0 *and* U_{next}*, defined in (1.6-7) and Assumption 1.8, approximating the solution of (1.2), with* ν_j *pre and post smoothing steps on level* j*, satisfies*

$$\gamma_B \leq \sum_{j=0}^{J-1} [\frac{C_1 h_j \log(B/h_j)}{\epsilon \nu_j} + \frac{C_2}{\sqrt{\nu}_j}] \Pi_{i=0}^{j} (1 + \frac{C_0 h_i}{\epsilon \nu_i}). \tag{1.10}$$

In addition, let for any $0 < \gamma < 1$*, the number of smoothing steps* ν_j *on each level,* $j = 0, 1, 2, \ldots, J-1$*, satisfy*

$$\nu_j \geq [\frac{C_3 h_j}{\epsilon} \frac{J \log(B/h_j)}{\gamma} + \frac{C_4}{\gamma^2}]. \tag{1.11}$$

Then the damping

$$\gamma_B \leq \gamma$$

holds. The work of this V-cycle is of the order $N \log^2 N$ *provided the number of degrees of freedom in the finest space* V_0 *is* N *and*

$$h_0 \sim \epsilon. \tag{1.12}$$

The constants $C_i, i = 0, \ldots, 4$*, are independent of* γ_B*,* J*,* h_j *and* ϵ*.*

Remark. The assumption $h_0 \geq 3\epsilon$ can, with small notational changes in the proof, be replaced by $h_0 \geq c_0 \epsilon$, where c_0 is a positive constant of order one.

Remark. As predicted from Theorem 1.1, the damping $\gamma(1)$, in Fig. 1, can be made smaller than 1 by increasing the number of smoothing steps.

In Section 7.1 we discuss the case when the characteristic is not aligned with the mesh, showing that the damping can be mesh dependent. The numerical experiments in Section 7.9 show that the exponential increase of the number of smoothing steps on coarser meshes, suggested by the Theorem 1.1, improves the convergence of the multigrid method for the

ETNA
Kent State University
etna@mcs.kent.edu

compressible Navier-Stokes equations in two space dimensions, as compared to the same amount of work with constant number of smoothing steps on each level.

Theorem 1.1 says that if we start with a residual supported in $[-B, B] \times R$, then one V-cycle will decrease the $L_1([-B, B] \times R)$ norm of the residual, by a factor γ_B. Besides confirming Experiment I in Fig. 1, one would like to use the theorem to prove that the multigrid method converges. However, we can not directly draw this conclusion from Theorem 1.1. Our proof of Theorem 1.1 is based on Fourier methods suitable to unbounded domains, and in an unbounded domain, the $L_1(R \times R)$-norm damping γ_∞ of the V-cycle becomes unbounded due to the factor $\log(B/h_j)$ in (1.10). Therefore, to prove that a V-cycle forms an L_1-contraction of the residual, we need to study bounded domains and boundary effects. If the damping (1.10) holds in a bounded domain, the V-cycle would form an L_1 contraction for the residual and the multigrid method would converge, provided sufficiently many smoothing steps are used. In addition to the numerical experiments, a further motivation that including boundary conditions does not change the behavior of the damping (1.10) is given in Section 9, Theorem 9.1, where the residual damping of a continuous version of the two grid method in the domain $(-\infty, 0) \times R$ is shown to give a contraction. This analysis is based on explicit solutions of a certain convection diffusion problem with variable coefficients. These explicit solutions are obtained by the Hopf-Cole transformation for the Burgers equation and are crucial also for treating the shock wave problem in Section 8. The iteration error can be obtained from the residual using the stability of the problem, again based on Green's functions as described in Section 7.5.

It remains to find a convergence proof of the multigrid method for convection diffusion problems in the fully discrete case including boundary conditions. Our analysis could be a first step in understanding some ingredients in such multigrid convergence. An other interesting open question is to prove multigrid convergence for convection problems with more sophisticated smoothers, such as the Gauss-Seidel method combined with proper ordering of the nodes. Gauss-Seidel smoothers can treat the case $\epsilon \ll h_0$, where the Jacobi smoother is very inefficient; see Fig. 5 in Section 8.

In Section 8, we study the convection-diffusion problem

$$\mathcal{L}w \equiv (u(x_1)w)_{x_1} - \epsilon \Delta w = 0, \tag{1.13}$$

which is the linearization of the two dimensional Burgers equation

$$\begin{aligned} &(\tfrac{u^2}{2})_{x_1} - \epsilon \Delta u = 0, \;\; x = (x_1, x_2) \in \boldsymbol{R}^2, \\ &u(\pm\infty, \cdot) = \mp 1, \end{aligned} \tag{1.14}$$

with the solution $u(x_1) = -\tanh \frac{x_1}{2\epsilon}$. We consider for the problem (1.13) a continuous version of a two grid method on V_ϵ and $V_{2\epsilon}$, with the isotropic diffusion $\epsilon\Delta$ and $2\epsilon\Delta$, respectively. This continuous two grid method is obtained by replacing the discrete smoothing operator by its zero mesh size limit. In Section 8, we prove

THEOREM 1.2. *Assume that the residual error $\mathcal{L}U_0$ initially is localized in the shock wave region B, i.e. $\mathcal{L}U_0(x) = 0$ for $x \notin B \equiv \{(x_1, x_2) \in \boldsymbol{R}^2 : |x_1| \leq Ch_0\}$. Then one iteration of the continuous two-grid cycle, with ν pre and post smoothing steps, damps the residual with a factor*

$$\gamma_B = \frac{\|\mathcal{L}U_{next}\|_{L_1(\boldsymbol{R}^2)}}{\|\mathcal{L}U_0\|_{L_1(\boldsymbol{R}^2)}} \leq \frac{1}{2} + \frac{C}{\nu}.$$

The proof is based on an explicit Green's function of the two dimensional variable coefficient problem (1.13), which after a separation of variables is obtained from the Hopf-Cole

ETNA
Kent State University
etna@mcs.kent.edu

transformation. The Green's function is then used to evaluate the residual both in the smoothing and in the correction problem. The damping in Theorem 1.2 has an interesting lower bound $1/2$, which is confirmed by our numerical experiments in Fig. 5 in Section 8, based on an experiment with the nonlinear multigrid method applied to (1.14).

Multigrid methods are widely used for solving fluid dynamics problems numerically; see [7], [18], but for convection dominated problems there exists as yet no satisfactory convergence theory for these multigrid methods. The convergence of multigrid iterations is related to the propagation and damping of the perturbations in the approximated equation. In convection dominated problems, the behavior of perturbations depends on the particular solution and the approximating scheme in a more distinct way than for elliptic problems, where the multigrid theory is well developed; see [5]. For instance for flow problems:

(A) the stability requires a mesh size dependent artificial diffusion, causing the discrete equations to vary with the grid.

(B) the damping is different inside and outside the shock regions.

If the equation (1.1) is solved without artificial diffusion and by a pure Galerkin method, then the multigrid method converge if and only if the coarsest mesh T^{h_J} is fine enough, i.e $h_J \leq C\epsilon$; see [1], [6], [12], [17]. Consequently, the exact coarse grid problem is in fact an expensive problem to solve for small ϵ. We have complete freedom in choosing suitable correction problems as long as they yield satisfactory convergence results. For stability reasons, it is natural to study correction steps where the bilinear form is based on a stable method for convection problems, e.g. the streamline diffusion method (1.2), or the first order accurate method with isotropic artificial diffusion $\frac{1}{2}(h_j \nabla U, \nabla v)$ replacing $\frac{1}{2}(h_j U_{x_1}, v_{x_1})$ in (1.2). These two examples of stable bilinear forms are mesh size dependent and hence different from the fine space form $a_0(\cdot,\cdot)$. Therefore, they cause an additional first order artificial diffusion error in a multigrid method based on corrections of type (1.6b).

For meshes with $h_j < 3\epsilon$ the streamline diffusion modification $\frac{1}{2}(h_j u_{x_1}, v_{x_1})$ should be omitted in (1.2). Following this simplification, the solution procedure is a standard Galerkin finite element method and requires $h_J < C\epsilon$, i.e. that the coarse mesh is sufficiently fine. To reduce the work of the coarsest correction problems one must have $h_J \gg \epsilon$. Our assumption, that $h_0 \geq 3\epsilon$ in Theorem 1.1, restricts the study to the behavior of multigrid methods in the convection dominated case, which in particular is important for coarse meshes. It also requires one to solve the exact "coarse" grid problem for the standard Galerkin method above with small ϵ. The conditions (1.11) and (1.12) ensure us that the residual damping does not deteriorate as $\epsilon \to 0$ and that the work is of almost optimal order.

The problem that the bilinear forms change with the mesh levels can be avoided by adding the same amount of artificial diffusion $h_J\Delta$ on all levels, thereby causing an artificial diffusion error of order h_J. For h_J of order h_0, the scheme is still first order accurate and the multigrid method converges; see [2]. In case of several levels, e.g. $h_J \sim 1$, the bilinear form must change with the levels otherwise the accuracy will be insufficient.

Numerical experiments with the multigrid method for the problem (1.1) based on the first order accurate diffusion converge slightly slower than the method based on the streamline diffusion; we discuss the reason of this behavior in Section 7.2.

The convergence analysis in the proof of Theorem 1.1 that treats the aspect (A), and the behavior of the damping (B) for a two-dimensional shock wave is studied in Theorem 1.2. In particular, we see that the residual is damped faster inside than outside the shock wave region for the two grid method using isotropic artificial diffusion.

In one space dimension the bilinear forms, corresponding to (1.1), are the same for the streamline diffusion method and the first order accurate artificial diffusion method, and the convergence of the two grid method was proved by Hackbush [16], both for periodic and

ETNA
Kent State University
etna@mcs.kent.edu

Dirichlet boundary conditions. Reusken's work [24] was the first to prove convergence of a two grid method for (1.1) in two space dimensions with changing bilinear form. The correction problem in his method is based on Schur complements and the smoothing operator is a block Jacobi iteration on $\{\text{fine nodes}\} \setminus \{\text{coarse nodes}\}$ with exact inversion of a block (this is related to ordering the nodes). His proof uses periodic boundary conditions and Fourier analysis.

Our analysis of the smoothing problem involves considering the smoothing iterations as a time stepping scheme, and yields that a sufficient number of smoothing steps is required to damp the residual; see the related previous works [3], [22]. Our use of the Galerkin orthogonality in the correction problem was inspired by [3] and the work [4] on a posteriori error estimates of multigrid methods.

2. A representation formula for multigrid iterations. In this section we derive an error representation of the iterations in a V-cycle method, based on the smoothing and correction steps for the error. We start by defining $\widetilde{U}$ to be the iteration error in the multigrid method, i.e.

$$\widetilde{U} \equiv \bar{U} - U, \tag{2.1}$$

where U is the exact discrete solution of (1.2) and $\bar{U}$ is the V-cycle iterate based on (1.3) and (1.6). Expressed in the $\widetilde{U}$-variable, the smoothing on the finest level can be written, $m = 0, 1, \ldots, \nu_0 - 1$,

$$\begin{aligned} \widetilde{U}_0 &= U_0 - U, \\ \widetilde{U}_{m+1}(x_i) &= \widetilde{U}_m(x_i) - ch_0 L_0 \widetilde{U}_m(x_i), \quad x_i \in \mathcal{N}_0, \end{aligned} \tag{2.2}$$

where the residual error is defined by

$$L_j \widetilde{U}(x_i) \equiv \frac{1}{h_j^2} a_j(\widetilde{U}, \phi_i), \text{ for } j = 0, 1, 2, \ldots, J, \tag{2.3}$$

for the basis functions $\phi_i \in \mathcal{B}_j$, satisfying (1.4). The correction $P_1 \widetilde{U}_{\nu_0} \in V_1$, of $\widetilde{U}_{\nu_0} \in V_0$, on the finest level yields the new approximation of the error $\widetilde{U}$

$$\widetilde{U}_{\nu_0} - P_1 \widetilde{U}_{\nu_0},$$

where the operator $P_{j+1} : V_0 \to V_{j+1}$ is defined by

$$a_{j+1}(P_{j+1}\widetilde{U}_{\nu_j}, v) = a_j(\widetilde{U}_{\nu_j}, v) \quad \forall v \in V_{j+1}, \text{ for } j = 0, 1, 2, \ldots, J-1. \tag{2.4}$$

The correction step (1.6) at level $j = 0$ is in the multigrid method solved approximately, in two steps. In the first step we smooth on the level 1, $m = 0, 1, \ldots, \nu_1 - 1$,

$$\begin{aligned} d_0 &= 0, \\ d_{m+1}(x_i) &= d_m(x_i) - ch_1[L_1 d_m(x_i) - \tfrac{1}{h_1}(a_0(\bar{U}_{\nu_0}, \phi_i) - (F, \phi_i + \tfrac{h_0}{2}\phi_{i,x_1}))] \\ &= d_m(x_i) - ch_1[L_1 d_m(x_i) - \tfrac{1}{h_1} a_0(\widetilde{U}_{\nu_0}, \phi_i)], \quad x_i \in \mathcal{N}_1. \end{aligned} \tag{2.5}$$

Define the correction error $\widetilde{d}$ by

$$\widetilde{d}_m \equiv -d_m + P_1 \widetilde{U}_{\nu_0}. \tag{2.6}$$

By (2.4) and (2.5) we have

$$\begin{aligned} \widetilde{d}_0 &= P_1 \widetilde{U}_{\nu_0}, \\ \widetilde{d}_{m+1}(x_i) &= \widetilde{d}_m(x_i) - ch_1 L_1 \widetilde{d}_m(x_i), \quad x_i \in \mathcal{N}_1. \end{aligned}$$

ETNA
Kent State University
etna@mcs.kent.edu

We note that the correction error $\widetilde{d}$ satisfies a similar smoothing condition on level $j = 1$ as the error $\widetilde{U}$ does on the finer level. In the second step, d, and hence also $\widetilde{d}$, is mapped to the coarser mesh analogous, to the correction of $\widetilde{U}$ on the finer level, i.e.

$$a_2(P_2\widetilde{d}_{\nu_1}, v) = a_1(\widetilde{d}_{\nu_1}, v) \quad \forall v \in V_2. \tag{2.7}$$

Therefore, we see that the evolution of the correction error $\widetilde{d}$ is described by $\widetilde{d}_{\nu_1} = S_{1,0}\widetilde{d}^{(1)}$, where $\widetilde{d}^{(j)}$ is given by

$$\widetilde{d}^{(j+1)} \equiv P_{j+1}S_{j,0}\widetilde{d}^{(j)}, \quad \widetilde{d}^{(0)} = \widetilde{U}_0 \text{ for } j = 0, 1, 2, \ldots, J-1. \tag{2.8}$$

Thus, the three grid approximation d_2^* of the correction d in (1.6), obtained by (2.6-8), has the representation

$$d_2^* = -\widetilde{d}_{\nu_1} + P_1\widetilde{U}_{\nu_0} + P_2\widetilde{d}_{\nu_1} = -S_{1,0}\widetilde{d}^{(1)} + P_1S_{0,0}\widetilde{d}^{(0)} + P_2S_{1,0}\widetilde{d}^{(1)}.$$

Analogously, by recursively applying (2.5-8) we obtain the multigrid approximation d_J^* of the two grid correction d defined in (1.6). The multigrid V-cycle without post smoothing, applied to the error $\widetilde{U}$ and starting with $\widetilde{U}_0$ in (2.2) has the following error after one iteration

$$\begin{aligned} \widetilde{U}_{\text{next}}^{\text{pre}} &= S_{0,0}\widetilde{U}_0 - d_J^* \\ &= (S_{0,0} - P_1S_{0,0})\widetilde{d}^{(0)} + (S_{1,0} - P_2S_{1,0})\widetilde{d}^{(1)} + \ldots + (S_{J-1,0} - P_JS_{J-1,0})\widetilde{d}^{(J-1)} \\ &= \sum_{j=0}^{J-1}(I - P_{j+1})S_{j,0}\widetilde{d}^{(j)}, \end{aligned} \tag{2.9}$$

where J is the coarsest grid level. We have used that the correction in V_J is solved exactly. The correction error $\widetilde{d}^{(j)}$ evolves with smoothing and mapping onto coarser and coarser meshes according to (2.8). By including post smoothing, the error $\widetilde{U}_{\text{next}}$ after one V-cycle is

$$\widetilde{U}_{\text{next}} = \sum_{j=0}^{J-1}\bar{S}_j(I - P_{j+1})S_{j,0}\widetilde{d}^{(j)}, \tag{2.10}$$

where

$$\bar{S}_j \equiv \Pi_{0\le i\le j}S_{i,0} \equiv S_{0,0}S_{1,0}\ldots S_{j,0}. \tag{2.11}$$

3. Green's functions and an overview of the proof. In this section, we first give a representation of the iteration error $\widetilde{U}$ and the residual $L_0\widetilde{U}$, defined in (2.3), in terms of a Green's function related to the problem (1.2). Then in the end of the section we present an overview of the proof of Theorem 1.1.

3.1. Green's functions for the V-cycle. Let for a given U_0 and $\widetilde{U}_0 \equiv U_0 - U$, the residual R be given by

$$L_0(\widetilde{U}_0)(x_i) = R(x_i) \quad \forall x_i \in \mathcal{N}_0, \tag{3.1}$$

and define, for a fixed $x_i \in \mathcal{N}_0$, the discrete Green's function $\xi(\cdot\,; x_i) \in V_0$ satisfying

$$L_0\xi(x_l; x_i) = \delta(x_l - x_i), \ \forall x_l \in \mathcal{N}_0, \tag{3.2}$$

ETNA
Kent State University
etna@mcs.kent.edu

where δ is the discrete Dirac function

$$\delta(x_k) = \begin{cases} 1/h_0^2, & x_k = 0, \\ 0, & x_k \neq 0, \end{cases} \quad x_k \in \mathcal{N}_0. \tag{3.3}$$

Equations (3.1) and (3.2) imply by a discrete Duhamels principle that

$$\widetilde{U}_0(x_l) = \sum_{x_i \in \mathcal{N}_0} R(x_i)\xi(x_l; x_i)h_0^2,$$

and

$$L_0\widetilde{U}_0(x_l) = \sum_{x_i \in \mathcal{N}_0} R(x_i)L_0\xi(x_l; x_i)h_0^2 = R(x_\ell).$$

The corresponding smoothing steps for the ξ variable on the finest level satisfy

$$\begin{aligned} \xi_0 &= \xi(\cdot\,; x_i), \\ \xi_{m+1}(x_k) &= \xi_m(x_k) - ch_0L_0\xi_m(x_k), \quad m = 0, 1, \ldots, \nu_0 - 1. \end{aligned} \tag{3.4}$$

Therefore, we have

$$\widetilde{U}_m(x_l) = \sum_{x_i \in \mathcal{N}_0} R(x_i)\xi_m(x_l; x_i)h_0^2,$$

and

$$L_0\widetilde{U}_{\nu_0}(x_l) = \sum_{x_i \in \mathcal{N}_0} R(x_i)L_0\xi_{\nu_0}(x_l; x_i)h_0^2.$$

The exactly solved correction step (1.6) yields

$$a_0(\xi_{\nu_0}, v) = a_1(P_1\xi_{\nu_0}, v) \quad \forall v \in V_1.$$

Hence, the two grid method has the residual

$$L_0(\widetilde{U}_{\nu_0} - P_1\widetilde{U}_{\nu_0})(x_l) = \sum_{x_i \in \mathcal{N}_0} R(x_i)L_0(\xi_{\nu_0} - P_1\xi_{\nu_0})(x_l; x_i)h_0^2.$$

In the multigrid method (2.5-8), with J correction levels, we obtain as in (2.9) and (2.10)

$$\begin{aligned} L_0(\widetilde{U}^{\text{pre}}_{\text{next}})(x_l) &= \sum_{j=0}^{J-1} \sum_{x_i \in \mathcal{N}_0} R(x_i)L_0(\xi^{(j)}_{\nu_j} - P_{j+1}\xi^{(j)}_{\nu_j})(x_l; x_i)h_0^2, \\ L_0(\widetilde{U}_{\text{next}})(x_l) &= \sum_{j=0}^{J-1} \sum_{x_i \in \mathcal{N}_0} R(x_i)L_0\bar{S}_j(\xi^{(j)}_{\nu_j} - P_{j+1}\xi^{(j)}_{\nu_j})(x_l; x_i)h_0^2, \end{aligned} \tag{3.5}$$

provided $\xi^{(j)}$ is defined as $\widetilde{d}^{(j)}$ in (2.8), i.e.,

$$\xi_0^{(j+1)} = P_{j+1}\xi^{(j)}_{\nu_j}, \quad \xi^{(j)}_{\nu_j} = S_{j,0}\xi_0^{(j)}, \quad \xi_0^{(0)} = \xi_0, \quad j = 0, 1, 2, \ldots, J-1. \tag{3.6}$$

Below we shall use the L_2-projection $\widetilde{\Pi}_{j+1} : L_2(\Omega) \to V_{j+1}$ defined by

$$\int_\Omega v\widetilde{\Pi}_{j+1}w dx = \int_\Omega vw dx \quad \forall v \in V_{j+1}. \tag{3.7}$$

ETNA
Kent State University
etna@mcs.kent.edu

Our next step is to estimate the discrete ℓ_1-norm of the right hand side in (3.5) using that for $w \in V_0$

$$\|w\|_{\ell_1} \equiv \sum_{x_i \in \mathcal{N}_0} |w(x_i)| h_0^2. \tag{3.8}$$

By combining the definition (2.3), the correction equation (2.4) and (3.6), (3.7) we obtain the following representation formula

$$\begin{aligned}
&L_0(\widetilde{U}_{\text{next}}^{\text{pre}})(x_l) = \textstyle\sum_{j=0}^{J-1} \sum_{x_i \in \mathcal{N}_0} R(x_i) L_0(\xi_{\nu_j}^{(j)} - P_{j+1}\xi_{\nu_j}^{(j)})(x_l; x_i) h_0^2 \\
&= \textstyle\sum_{j,i} [(a_j(\xi_{\nu_j}^{(j)}, \phi_l) - a_{j+1}(P_{j+1}\xi_{\nu_j}^{(j)}, \phi_l)) \\
&\quad + (\tfrac{1}{2}(h_0 - h_j)\xi_{\nu_j,x_1}^{(j)}, \phi_{l,x_1}) - (\tfrac{1}{2}(h_0 - h_{j+1}) P_{j+1}\xi_{\nu_j,x_1}^{(j)}, \phi_{l,x_1})] R(x_i) \\
&= \textstyle\sum_{j,i} [a_j(\xi_{\nu_j}^{(j)}, (I - \widetilde{\Pi}_{j+1})\phi_l) - a_{j+1}(P_{j+1}\xi_{\nu_j}^{(j)}, (I - \widetilde{\Pi}_{j+1})\phi_l) \\
&\quad + (\tfrac{1}{2}(h_0 - h_j)\xi_{\nu_j,x_1}^{(j)}, \phi_{l,x_1}) - (\tfrac{1}{2}(h_0 - h_{j+1})(P_{j+1}\xi_{\nu_j}^{(j)})_{x_1}, \phi_{l,x_1})] R(x_i) \\
&= \textstyle\sum_{j,i} [((\xi_{\nu_j,x_1}^{(j)} - P_{j+1}\xi_{\nu_j,x_1}^{(j)}), (I - \widetilde{\Pi}_{j+1})\phi_l) \\
&\quad - (\widetilde{D}_{x_1}^2((\tfrac{h_j}{2} + \epsilon)\xi_{\nu_j}^{(j)} - (\tfrac{h_{j+1}}{2} + \epsilon) P_{j+1}\xi_{\nu_j}^{(j)}), (I - \widetilde{\Pi}_{j+1})\phi_l) \\
&\quad - (\epsilon \widetilde{D}_{x_2}^2(\xi_{\nu_j}^{(j)} - P_{j+1}\xi_{\nu_j}^{(j)}), (I - \widetilde{\Pi}_{j+1})\phi_l) \\
&\quad - (\tfrac{1}{2}(h_0 - h_j)\widetilde{D}_{x_1}^2 \xi_{\nu_j}^{(j)}, \phi_l) + (\tfrac{1}{2}(h_0 - h_{j+1})\widetilde{D}_{x_1}^2 P_{j+1}\xi_{\nu_j}^{(j)}, \phi_l)] R(x_i),
\end{aligned} \tag{3.9}$$

where we use the following notation for discrete second order derivatives

$$\widetilde{D}_{x_k}^2 : V_0 \to V_0 \quad (-\widetilde{D}_{x_k}^2 w, v) = (w_{x_k}, v_{x_k}) \quad \forall v \in V_0, \;\; k = 1, 2. \tag{3.10}$$

Let

$$\frac{h_j^*}{2} = \frac{h_j}{2} + \epsilon,$$

which by the assumption $h_0 \geq 3\epsilon$ in Theorem 1.1 implies

$$h_j^* = C_j h_j.$$

For notational simplicity we consider $C_j = 1$, which by the assumption $h_0 \geq 3\epsilon$ corresponds to the neglectable change of replacing $h_j/2$ by $h_j/2 - \epsilon$ in the streamline diffusion parameter. Hereafter, the superscript $*$ is omitted.

Now defining the discrete residual $\widetilde{L}_j \xi_{\nu_j}^{(j)} \in V_0$ by

$$(\widetilde{L}_j \xi_{\nu_j}^{(j)}, v) = a_j(\xi_{\nu_j}^{(j)}, v) \quad \forall v \in V_0,$$

we can rewrite the residual

$$\begin{aligned}
&L_0(\widetilde{U}_{\text{next}}^{\text{pre}})(x_l) \\
&= \textstyle\sum_{j=0}^{J-1} \sum_{x_i \in \mathcal{N}_0} [(\widetilde{L}_j \xi_{\nu_j}^{(j)}, (I - \widetilde{\Pi}_{j+1})\phi_l) - (\widetilde{L}_{j+1} P_{j+1}\xi_{\nu_j,x_1}^{(j)}, (I - \widetilde{\Pi}_{j+1})\phi_l) \\
&\quad - (\tfrac{1}{2}(h_0 - h_j)\widetilde{D}_{x_1}^2 \xi_{\nu_j}^{(j)}, \phi_l) + (\tfrac{1}{2}(h_0 - h_{j+1})\widetilde{D}_{x_1}^2 P_{j+1}\xi_{\nu_j}^{(j)}, \phi_l)] R(x_i).
\end{aligned} \tag{3.11}$$

It turns out that one single pre smoothing V-cycle can not make the residual quotient in (1.9) small, however, two V-cycles will damp the residual. We discuss this in more detail in Section 7.8. The mechanism of the damping in the second iteration is similar to the reason

ETNA
Kent State University
etna@mcs.kent.edu

why one V-cycle with pre and post smoothing damps the residual. Let us now study the case with post smoothing. In order to use the correction equations (2.3), we shall assume that the smoothing operator defined in (2.11),

$$\bar{S}_j \equiv \Pi_{0\le i\le j} S_{i,0}$$

is translation invariant, which is the case for a uniform mesh and the constant coefficient problem (1.2) studied here. The post smoothing operator is a convolution

$$\bar{S}_j v(x_k) = \sum_{y_i\in\mathcal{N}_0} \bar{g}_j(y_i) v(x_k - y_i) \equiv \bar{g}_j * v(x_k), \quad \forall v \in V_0,\ x_k \in \mathcal{N}_0, \tag{3.13}$$

for a certain function $\bar{g}_j$, which will be studied in detail in Section 4. The translation invariance implies that

$$\begin{aligned} a_j(\bar{S}_j\xi^{(j)}, \phi_l) &= \sum_{y_i\in\mathcal{N}_0} \bar{g}_j(y_i) a_j(\xi^{(j)}(\cdot - y_i), \phi_l) \\ &= \sum_{y_i\in\mathcal{N}_0} \bar{g}_j(y_i) a_j(\xi^{(j)}, \phi_l(\cdot + y_i)) = a_j(\xi^{(j)}, \bar{g}_j(-\cdot) * \phi_l), \end{aligned} \tag{3.14}$$

and similarly for $\bar{S}_j P_{j+1}\xi^{(j)}$. As in (3.9) we obtain by (3.14) the residual error representation

$$\begin{aligned} L_0(\widetilde{U}_{\text{next}})(x_l) &= \sum_{j=0}^{J-1} \sum_{x_i\in\mathcal{N}_0} a_j(\xi_{\nu_j}^{(j)}, (I - \widetilde{\Pi}_{j+1})\bar{g}_j(-\cdot) * \phi_l) R(x_i) \\ &\quad - \sum_{j,i} a_{j+1}(P_{j+1}\xi_{\nu_j}^{(j)}, (I - \widetilde{\Pi}_{j+1})\bar{g}_j(-\cdot) * \phi_l) R(x_i) \\ &\quad + \sum_{j,i} \frac{1}{2}(h_0 - h_j)(\xi_{\nu_j,x_1}^{(j)}, \bar{g}_j(-\cdot) * \phi_{l,x_1}) R(x_i) \\ &\quad - \sum_{j,i} \frac{1}{2}(h_0 - h_{j+1})((P_{j+1}\xi_{\nu_j}^{(j)})_{x_1}, \bar{g}_j(-\cdot) * \phi_{l,x_1}) R(x_i). \end{aligned} \tag{3.15}$$

In Section 8, we derive a similar representation for the residual in a linearized shock wave problem, which is not translation invariant.

Our goal is to estimate the ℓ_1-norms of the sums in equality (3.15) by using the properties of the smoothing operator $S_{j,0}$ in (1.3), (2.2) and the correction operator P_j in (2.4). This is carried out in three steps. First, the smoothing operator is analyzed by Fourier methods in Section 4. Then, in Section 5, the correction operator is studied, also using Fourier analysis. Finally, in Section 6, we combine the results of Sections 4 and 5 to estimate the residual in (3.15) and thereby prove Theorem 1.1.

3.2. Overview of the proof. Let us first give a heuristic motivation that (3.15) implies the damping of the V-cycle in Theorem 1.1. This motivation also gives the basic structure and idea of the proof of Theorem 1.1, which is an extension of this overview, based on differential operators, to discrete operators. The proof has the three steps: Evolution of the smoothing problem, estimates of the correction problem, and residual error estimates.

Evolution of the smoothing. In Section 4, we shall see that the following parabolic problem reflects the behavior of the smoothing (3.6) at level j

$$\xi_t + c h_j L_j \xi = 0, \quad 0 < t < \nu_j, \tag{3.16}$$

ETNA
Kent State University
etna@mcs.kent.edu

where

$$L_j\xi \equiv \xi_{x_1} - \frac{h_j}{2}\xi_{x_1x_1} - \epsilon\xi_{x_2x_2}.$$

Let $X \equiv L_j\xi$, then

$$X_t + ch_jL_jX = 0, \quad 0 < t < \nu_j, \tag{3.17}$$

and by (3.2) we have $X(x,0) = \delta(x - x_i)$ initially at level zero, where for simplicity x_i is chosen as the origin. The solution of (3.17) on the finest level $j = 0$ is a Gaussian

$$X(x,t) = \frac{\exp[-(x_1 - ch_jt)^2/(cth_j^2) - x_2^2/(2tch_j\epsilon)]}{\sqrt{2}\pi tch_j^{3/2}\epsilon^{1/2}}. \tag{3.18}$$

In the correction step, the Gaussian is mapped to the coarser mesh having twice the mesh size. Assume that $\nu_j > h_j/\epsilon$, cf. (1.11), then the Gaussian is well resolved on the coarser mesh and therefore the mapping to the coarser mesh yields a neglectable change. Hence, $X(\cdot,\nu_j)$ in (3.18) is a good approximation of $L_j\xi^{(j)}$ also at the next levels $j > 0$.

The correction problem. To estimate the three parts $\xi_{x_1}, h_j\xi_{x_1x_1}$ and $\epsilon\xi_{x_2x_2}$ of the residual, we solve for ξ in

$$L_j\xi = X(\cdot\,,\nu_j). \tag{3.19}$$

Then we obtain ξ as a new approximate Gaussian

$$\xi((x_1,x_2),\nu_j) \sim \begin{cases} \exp[-x_2^2/(4c\epsilon x_1)]/\sqrt{4\pi\epsilon x_1} & \text{if } x_1 > h_j\sqrt{\nu}_j, \\ \exp[-c_1|x_1|/h_j - x_2^2/(4c\epsilon h_j)]/\sqrt{c_2\epsilon h_j} & \text{if } x_1 < h_j\sqrt{\nu}_j. \end{cases} \tag{3.20}$$

Residual error estimates. By the expression (3.20) for ξ we can estimate the residual error caused by the artificial diffusion part of (3.15)

$$\int_{x_1>h_j\sqrt{\nu}_j}\int_{-\infty}^{\infty} h_j|\xi_{x_1x_1}|dx_1dx_2 \le C\int_{x_1>h_j\sqrt{\nu}_j}^{\infty} h_j/x_1^2dx_1 = \frac{C}{\sqrt{\nu}_j}. \tag{3.21}$$

To estimate the projection part $a_j(\xi,(I-\widetilde{\Pi}_{j+1})\bar{g}_j(-\,\cdot)*\phi_l)$, we first use

$$\int_{-B}^{B}\int_{\mathbb{R}}(|\xi_{x_1}| + h_j|\xi_{x_1x_1}| + \epsilon|\xi_{x_2x_2}|)dx \le C\log\frac{B}{h_j}, \tag{3.22}$$

which follows similarly to (3.21). Then, standard error estimates of the L_2-projection (3.7) yield

$$\|(I-\widetilde{\Pi}_{j+1})\bar{g}_j\|_{L_1} \le Ch_{j+1}^2\|\bar{g}_j\|_{W_1^2}, \tag{3.23}$$

where W_1^2 denotes the Sobolev space of functions with two derivates in $L_1(\mathbb{R}^2)$. The definition (3.13) implies that $\bar{g}_j \sim X(\cdot\,,\nu_j)$, so that by (3.22), (3.18), (3.23) and the fact $\sum_{\phi_l\in\mathcal{B}_0}\phi_l = 1$ we have

$$\begin{aligned} &\|a_j(\xi,(I-\widetilde{\Pi}_{j+1})\bar{g}_j*\phi_\cdot)\|_{\ell_1((-B,B)\times\mathbb{R})} \\ &\quad\le \|(I-\widetilde{\Pi}_{j+1})\bar{g}_j\|_{\ell_1}\int_{-B}^{B}\int_{\mathbb{R}}(|\xi_{x_1}| + h_j|\xi_{x_1x_1}| + \epsilon|\xi_{x_2x_2}|)dx \\ &\quad\sim Ch_{j+1}^2\|X(\cdot\,,\nu_j)\|_{W_1^2}\log\tfrac{B}{h_j} \le \tfrac{Ch_j}{\epsilon\nu_j}\log\tfrac{B}{h_j}. \end{aligned} \tag{3.24}$$

ETNA
Kent State University
etna@mcs.kent.edu

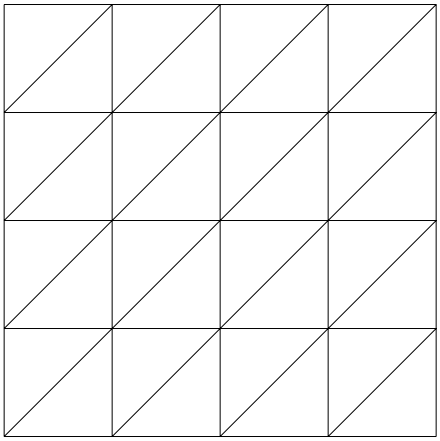

FIG. 4.1. *The uniform aligned mesh.*

By summation over $R(x_i)$ in (3.15) and combining (3.21), (3.24) we have heuristically motivated that (1.10) holds. In Sections 4, 5 and 6 we rigorously do the analogous analysis of (3.16-18), (3.19-20) and (3.21-24), respectively, for the discrete problem (1.2) in the case of $\Omega = \boldsymbol{R}^2$ and a uniform mesh.

4. ℓ_1-estimates of the Green's function in the smoothing problem. In this section, we follow the idea in (3.16-18) to estimate the residual in the smoothing problem. To obtain estimates of the smoothing and correction operators we simplify by assuming that the mesh is uniform and that $\Omega = \boldsymbol{R}^2$ is unbounded and hence excluding possible boundary effects; in Section 9 we include boundary conditions. We consider meshes $\mathcal{M}_j$ with nodal points

$$(n, m)h_j, \quad n, m \in \boldsymbol{Z}, \tag{4.1}$$

and edges in the direction $(1, 0)$, $(0, 1)$, $(1, 1)$, see Fig. 2. The mesh is in this case aligned to the characteristic direction $(1, 0)$. In Section 7.1, we treat a uniform mesh which is not aligned to the characteristic and thereby introduces fourth order dissipation in the cross wind direction, which improves the multigrid convergence.

4.1. The smoothing problem. In the first step, we study the evolution of the residual

$$X^{(j)}(x_i) \equiv L_j \xi^{(j)}(x_i), \quad x_i \in \mathcal{N}_j,$$

where by (2.3) and (4.1) $L_j : V_j \to V_j$, $X^{(j)} \in V_j$, is the finite difference operator with nodal values

$$\begin{aligned}(L_j X^{(j)})(h_j n, h_j m) = \tfrac{1}{h_j}[&X^{(j)}(h_j n, h_j m) - \tfrac{5}{6} X^{(j)}(h_j(n-1), h_j m) \\ &- \tfrac{1}{6} X^{(j)}(h_j(n+1), h_j m) - \tfrac{1}{6} X^{(j)}(h_j n, h_j(m+1)) + \tfrac{1}{6} X^{(j)}(h_j n, h_j(m-1)) \\ &- \tfrac{1}{6} X^{(j)}(h_j(n-1), h_j(m-1)) + \tfrac{1}{6} X^{(j)}(h_j(n+1), h_j(m+1))] \\ &+ \tfrac{\epsilon}{h_j^2}[-\tfrac{1}{4} X^{(j)}(h_j n, h_j(m+1)) + \tfrac{1}{2} X^{(j)}(h_j n, h_j m) - \tfrac{1}{4} X^{(j)}(h_j n, h_j(m-1))].\end{aligned} \tag{4.2}$$

For simplicity in the notation we have replaced $a_{h_j}(\cdot, \cdot)$ by $a_{h_j - 2\epsilon}(\cdot, \cdot)$, cf. (3.9). Taking the L_j difference quotient of $\xi^{(j)}$ in (3.4), we obtain the evolutionary problem

$$X_{k+1}^{(j)}(x_i) = X_k^{(j)}(x_i) - c h_j L_j X_k^{(j)}(x_i) \quad \forall x_i \in \mathcal{N}_j. \tag{4.3}$$

ETNA
Kent State University
etna@mcs.kent.edu

Let $\widehat{Z}$ be the Fourier transform of Z, i.e.

$$\begin{aligned}\widehat{Z}(\omega_1,\omega_2) &= h_j^2 \textstyle\sum_{n,m\in \boldsymbol{Z}} Z(h_jn,h_jm)\exp(i(n\omega_1+m\omega_2)h_j),\\ Z(h_jn,h_jm) &= (2\pi)^{-2}\textstyle\int_0^{2\pi/h_j}\int_0^{2\pi/h_j}\widehat{Z}(\omega_1,\omega_2)\exp(-i(n\omega_1+m\omega_2)h_j)d\omega_1 d\omega_2.\end{aligned}$$

Then the smoothing problem (4.3) transforms to

$$\begin{aligned}\widehat{X}_{k+1}^{(j)} = \ & \widehat{X}_k^{(j)} - c[1-\tfrac{5}{6}\exp(-ih_j\omega_1)-\tfrac{1}{6}\exp(ih_j\omega_1)-\tfrac{1}{6}\exp(ih_j\omega_2)+\tfrac{1}{6}\exp(-ih_j\omega_2)\\ & -\tfrac{1}{6}\exp(-ih_j\omega_1-ih_j\omega_2)+\tfrac{1}{6}\exp(ih_j\omega_1+ih_j\omega_2)+\tfrac{\epsilon}{h_j}(1-\cos(h_j\omega_2))]\widehat{X}_k^{(j)}.\end{aligned}$$

Therefore, the Green's function $g_j \in V_j$ of (4.3) for ν_j smoothing steps is

$$\begin{aligned}\widehat{g}_j = \ & (1-c[1-\tfrac{5}{6}\exp(-ih_j\omega_1)-\tfrac{1}{6}\exp(ih_j\omega_1)-\tfrac{1}{6}\exp(ih_j\omega_2)+\tfrac{1}{6}\exp(-ih_j\omega_2)\\ & -\tfrac{1}{6}\exp(-ih_j\omega_1-ih_j\omega_2)+\tfrac{1}{6}\exp(ih_j\omega_1+ih_j\omega_2)+\tfrac{\epsilon}{h_j}(1-\cos(h_j\omega_2))])^{\nu_j},\end{aligned} \tag{4.4}$$

which satisfies the ℓ_1-estimates of Lemma 4.1 below, to be used in Section 6 to estimate (3.15). Let D_{x_i} and $D_{x_i}^{(2)}$ denote the difference operators

$$\begin{aligned}&D_{x_i}, D_{x_i}^{(2)} : V_j \to V_j, \ \ i=1,2,\\ &e_1 \equiv (1,0),\ e_2 \equiv (0,1),\\ &D_{x_i}v(x) = \tfrac{v(x+h_je_i)-v(x)}{h_j},\\ &D_{x_i}^{(2)}v(x) = \tfrac{v(x+h_je_i)-2v(x)+v(x-h_je_i)}{h_j^2},\end{aligned} \tag{4.5}$$

and furthermore, let g_j be extended to $\boldsymbol{R}^2$ by $g_j \in V_j$.

LEMMA 4.1. *There is a constant C, independent of h_j and ϵ, such that*

$$\|g_j\|_{\ell_1} \equiv \textstyle\sum_{x_i\in\mathcal{N}_j}|g_j(x_i)|h_j^2 \le \ 1+\frac{Ch_j}{\epsilon\nu_j}, \tag{4.6}$$

$$h_j^2\|g_j\|_{w_1^2} \le \ \ \tfrac{Ch_j}{\epsilon\nu_j}, \tag{4.7}$$

$$\|\epsilon\widetilde{D}_{x_2}^{(2)}g_j\|_{\ell_1} + \|h_j\widetilde{D}_{x_1}^{(2)}g_j\|_{\ell_1} \le \ \tfrac{C}{h_j\nu_j}, \tag{4.8}$$

$$\|D_{x_1}g_j\|_{\ell_1} \le \ \tfrac{C}{h_j\sqrt{\nu_j}}, \tag{4.9}$$

where w_1^2 denotes the discrete version of the Sobolev space W_1^2, (defined below (3.23))

$$\|v\|_{w_1^2} \equiv \| \, |D_{x_1}^{(2)}v| + |D_{x_2}^{(2)}v| + |D_{x_1}D_{x_2}v| \, \|_{\ell_1}.$$

Proof. First we note that by (4.4)

$$\begin{aligned}&|\widehat{g}_j - \exp(-c(h_j^2\omega_1^2+\epsilon h_j\omega_2^2-h_j\omega_1 i)\nu_j)|\\ &\quad \le C(h_j^2\omega_1^2+\epsilon h_j\omega_2^2)^2\nu_j\exp(-c(h_j^2\omega_1^2+\epsilon h_j\omega_2^2)\nu_j).\end{aligned} \tag{4.10a}$$

ETNA
Kent State University
etna@mcs.kent.edu

Next, we split

$$g_j - \frac{\exp(-\frac{(x_1-c\nu_j h_j)^2}{4ch_j^2\nu_j} - \frac{x_2^2}{4c\epsilon h_j\nu_j})}{4\pi c\sqrt{\epsilon h_j^3\nu_j^2}} \tag{4.10b}$$

into near and far fields, N and F, respectively, where

$$\begin{aligned} N &= \{(x_1,x_2)\in\mathcal{N}_j : |x_1|\le\sqrt{h_j^2\nu_j}, |x_2|\le\sqrt{\epsilon h_j\nu_j}\},\\ F &= \mathcal{N}_j\setminus N. \end{aligned}$$

Then the ℓ_1-norm of (4.10b) can be estimated in terms of weighted ℓ_2-norms as follows

$$\begin{aligned} &\left\| g_j - \frac{\exp(-\frac{(x_1-c\nu_j h_j)^2}{4ch_j^2\nu_j} - \frac{x_2^2}{4c\epsilon h_j\nu_j})}{4\pi c\sqrt{\epsilon h_j^3\nu_j^2}} \right\|_{\ell_1}\\ &= \sum_N \left| g_j - \frac{\exp(-\frac{(x_1-c\nu_j h_j)^2}{4ch_j^2\nu_j} - \frac{x_2^2}{4c\epsilon h_j\nu_j})}{4\pi c\sqrt{\epsilon h_j^3\nu_j^2}} \right| h_j^2\\ &+ \sum_F \left| g_j - \frac{\exp(-\frac{(x_1-c\nu_j h_j)^2}{4ch_j^2\nu_j} - \frac{x_2^2}{4c\epsilon h_j\nu_j})}{4\pi c\sqrt{\epsilon h_j^3\nu_j^2}} \right| h_j^2\\ &\equiv I + II, \end{aligned} \tag{4.11}$$

where by Cauchy's inequality, Parseval's formula and (4.10a)

$$\begin{aligned} I &\le \left\| g_j - \frac{\exp(-\frac{(x_1-c\nu_j h_j)^2}{4ch_j^2\nu_j} - \frac{x_2^2}{4c\epsilon h_j\nu_j})}{4\pi c\sqrt{\epsilon h_j^3\nu_j^2}} \right\|_{\ell_2} \sqrt{\sum_N h_j^2}\\ &\le \left\| \widehat{g}_j - \exp(-c(h_j^2\omega_1^2 + \epsilon h_j\omega_2^2 - h_j\omega_1 i)\nu_j) \right\|_{L_2([0,2\pi/h_j]^2)} \sqrt{\sum_N h_j^2}\\ &\le C/\nu_j, \end{aligned}$$

$$\begin{aligned} II &\le \left\| [(\frac{x_1}{\sqrt{h_j^2\nu_j}})^2 + (\frac{x_2}{\sqrt{h_j\epsilon\nu_j}})^2] g_j - \frac{\exp(-\frac{(x_1-c\nu_j h_j)^2}{4ch_j^2\nu_j} - \frac{x_2^2}{4c\epsilon h_j\nu_j})}{4\pi c\sqrt{\epsilon h_j^3\nu_j^2}}) \right\|_{\ell_2}\\ &\qquad \times \sqrt{\sum_F [(\frac{x_1}{\sqrt{h_j^2\nu_j}})^2 + (\frac{x_2}{\sqrt{h_j\epsilon\nu_j}})^2]^{-2} h_j^2}\\ &\le \left\| [(\frac{\partial_{\omega_1}}{\sqrt{h_j^2\nu_j}})^2 + (\frac{\partial_{\omega_2}}{\sqrt{h_j\epsilon\nu_j}})^2] (\widehat{g}_j - \exp(-c(h_j^2\omega_1^2 + \epsilon h_j\omega_2^2 - h_j\omega_1 i)\nu_j)) \right\|_{L_2([0,2\pi/h_j]^2)}\\ &\qquad \times (2h_j^2\nu_j\epsilon h_j\nu_j)^{1/4} \le \tfrac{C}{\nu_j}. \end{aligned}$$

Moreover, the function $\exp(-c(h_j^2\omega_1^2 + \epsilon h_j\omega_2^2 - h_j\omega_1 i)\nu_j)$ is the Fourier transform of

$$\frac{\exp(-\frac{(x_1-c\nu_j h_j)^2}{4ch_j^2\nu_j} - \frac{x_2^2}{4c\epsilon h_j\nu_j})}{4\pi c\sqrt{\epsilon h_j^3\nu_j^2}},$$

ETNA
Kent State University
etna@mcs.kent.edu

which with our quadrature (3.8) has ℓ_1-norm less than $1 + Ch_j/(\epsilon\nu_j)$. Combining this with the estimates of I and II prove (4.6).

Next, to estimate (4.7) we proceed as above

$$\begin{aligned}
&\|h_j^2 D_{x_1}^{(2)} g_j\|_{\ell_1} \le \|h_j^2 D_{x_1}^{(2)} g_j\|_{\ell_2} \sqrt{\sum_N h_j^2} \\
&+ \left\| [(\tfrac{x_1}{\sqrt{h_j^2\nu_j}})^2 + (\tfrac{x_2}{\sqrt{h_j\epsilon\nu_j}})^2] h_j^2 D_{x_1}^{(2)} g_j \right\|_{\ell_2} \sqrt{\sum_F [(\frac{x_1}{\sqrt{h_j^2\nu_j}})^2 + (\frac{x_2}{\sqrt{h_j\epsilon\nu_j}})^2]^{-2} h_j^2} \qquad (4.12) \\
&\equiv I + II,
\end{aligned}$$

where

$$\begin{aligned}
|I| \le\ & C(1-\cos(\omega_1 h_j))\widehat{g}_j\|_{L_2} (h_j^3 \epsilon \nu_j^2)^{1/4} \le \tfrac{C}{\nu_j}, \\
|II| \le\ & C \left\| [(\tfrac{\partial_{\omega_1}}{\sqrt{h_j^2\nu_j}})^2 + (\tfrac{\partial_{\omega_2}}{\sqrt{h_j\epsilon\nu_j}})^2](1-\cos(\omega_1 h_j))\widehat{g}_j \right\|_{L_2} (h_j^3\epsilon\nu_j^2)^{1/4} \le \tfrac{C}{\nu_j},
\end{aligned}$$

which proves that the $D_{x_1}^{(2)}$ part of the w_1^2-norm satisfies (4.7). The proof of the $D_{x_2}^{(2)}$ and $D_{x_1}D_{x_2}$ parts follows as above.

To prove (4.8), we note that by (3.10)

$$\widetilde{D}_{x_1}^{(2)} g_j(x_l) = \sum_{x_i \in \mathcal{N}_0} M^{-1}(i) D_{x_1}^{(2)} g_j(x_l - x_i) \equiv M^{-1} * D_{x_1}^{(2)} g_j, \qquad (4.12')$$

where $M^{-1}(i) \equiv \widetilde{M}^{-1}(\cdot + i, \cdot)$ is the inverse of the mass matrix in V_0

$$\widetilde{M}(n,m) = \int_{\mathbb{R}^2} \phi_n \phi_m dx.$$

Since

$$\|M^{-1}\|_{\ell_1} \le C,$$

we have

$$\|\widetilde{D}_{x_1}^{(2)} g_j\|_{\ell_1} = \|M^{-1} * D_{x_1}^{(2)} g_j\|_{\ell_1} \le \|M^{-1}\|_{\ell_1} \|D_{x_1}^{(2)} g_j\|_{\ell_1} \le C \|D_{x_1}^{(2)} g_j\|_{\ell_1},$$

which by (4.12) proves that the second term of (4.8) satisfies the required bound. The estimate of the first term and (4.9) follows as (4.7). □

4.2. The correction problem. Our next step is to study the residual $a(\xi, \cdot)$ in the correction step

$$a_{j+1}(P_{j+1}\xi_{\nu_j}^{(j)}, v) = a_j(\xi_{\nu_j}^{(j)}, v) \quad \forall v \in V_{j+1}, \ \ \xi \in V_j. \qquad (4.13)$$

Let us therefore define the residuals $X^{(j)} \in V_j$ and $\bar{P}_{j+1}X^{(j)} \in V_{j+1}$ by

$$X^{(j)}(x_m) \equiv \frac{1}{h_j^2} a_j(\xi_{\nu_j}^{(j)}, \phi_m) \quad \forall x_m \in \mathcal{N}_j, \ \phi_m \in \mathcal{B}_j, \ \phi_m(x_m) = 1, \qquad (4.14)$$

$$(\bar{P}_{j+1}X^{(j)})(x_n) \equiv \frac{1}{h_{j+1}^2} a_{j+1}(P_{j+1}\xi_{\nu_j}^{(j)}, \bar{\phi}_n) \ \forall x_n \in \mathcal{N}_{j+1}, \bar{\phi}_n \in \mathcal{B}_{j+1}, \bar{\phi}_n(x_n) = 1. \qquad (4.15)$$

ETNA
Kent State University
etna@mcs.kent.edu

We note that the residual $X^{(j)}$ is the result of the smoothing (4.3). In the correction step, the residual is mapped to $\bar{P}_{j+1}X^{(j)}$ on the coarser grid. Our goal is now to express $\bar{P}_{j+1}X^{(j)}$ in terms of $X^{(j)}$. By (4.13-15) and since $\mathcal{B}_{j+1} \ni \bar{\phi}_n(x) = \sum_i \bar{\phi}_n(x_i)\phi_i(x),\ \phi_i \in \mathcal{B}_j$, we obtain

$$(\bar{P}_{j+1}X^{(j)})(x_n) = \sum_{x_i \in \mathcal{N}_j} \frac{h_j^2}{h_{j+1}^2}\bar{\phi}_n(x_i)X^{(j)}(x_i) \quad \forall x_n \in \mathcal{N}_{j+1}. \tag{4.16}$$

We have

$$\begin{aligned}
\sum_{\{i:\phi_i \in \mathcal{B}_j\}} \frac{h_j^2}{h_{j+1}^2}\bar{\phi}_n(x_i) &= 1 \quad \forall \bar{\phi}_n \in \mathcal{B}_{j+1}, \\
\sum_{\{n:\bar{\phi}_n \in \mathcal{B}_{j+1}\}} \bar{\phi}_n(x_i) &= 1,
\end{aligned}$$

which by (4.16) shows that the correction operator $\bar{P}$ does not increase the ℓ_1-norm

$$\begin{aligned}
&\|\bar{P}_{j+1}X^{(j)}\|_{\ell_1} = \sum_n h_{j+1}^2 |(\bar{P}_{j+1}X^{(j)})(x_n)| \\
&\leq \sum_n \sum_i |X^{(j)}(x_i)|\bar{\phi}_n(x_i)h_j^2 = \sum_i h_j^2 |X^{(j)}(x_i)| = \|X^{(j)}\|_{\ell_1}.
\end{aligned} \tag{4.17}$$

¿From our multigrid algorithm (3.5) and from the evolution of the Greens function $\xi^{(j)}$ in (3.6), we are led to study successive smoothing problems with initial data given by $\bar{P}_{j+1}$ corrections of the residual $L_j\xi^{(j)}$ smoothed on the finer mesh. Define

$$X^{(j)} \equiv L_j\xi^{(j)}.$$

Then the representation (3.6) implies that

$$\begin{aligned}
X^{(-1)} &= \delta, \\
X^{(j)} &= g_j(\bar{P}_j X^{(j-1)}), \quad j = 0, \ldots, J,
\end{aligned} \tag{4.18}$$

where $\bar{P}_j$ is given by (4.16), $\bar{P}_0 \equiv I$ and

$$g_j(\bar{P}_j X^{(j-1)}) = g_j * (\bar{P}_j X^{(j-1)}).$$

Here the operator $*$ denotes the convolution

$$w * v(x_i) = \sum_{y_n \in \mathcal{N}_j} w(x_i - y_n)v(y_n),$$

and the Green's function g_j is the j-level smoothing function defined in (4.4). Combining (4.13), (4.17), (4.18) and Lemma 4.1, we obtain

ETNA
Kent State University
etna@mcs.kent.edu

LEMMA 4.2. *There is a constant C, independent of J, h_j and ϵ, such that for $j \le J-1$*

$$\begin{aligned}
\|\bar{P}_{j+1}X^{(j)}\|_{\ell_1} &\le \Pi_{i\le j}(1+\frac{Ch_i}{\epsilon\nu_i}),\\
\|g_j(\bar{P}_jX^{(j-1)})\|_{\ell_1} &\le \Pi_{i\le j}(1+\frac{Ch_i}{\epsilon\nu_i}),\\
h_j^2(\|g_j(\bar{P}_jX^{(j-1)})\|_{w_1^2}+\|(\bar{P}_jX^{(j-1)})\|_{w_1^2}) &\le \tfrac{Ch_j}{\epsilon\nu_j}\Pi_{i\le j}(1+\frac{Ch_i}{\epsilon\nu_i}),\\
\|\epsilon\widetilde{D}^{(2)}_{x_2}g_j\bar{P}_{j+1}X^{(j)}\|_{\ell_1}+\|h_j\widetilde{D}^{(2)}_{x_1}g_j\bar{P}_{j+1}X^{(j)}\|_{\ell_1} &\le \tfrac{C}{h_j\nu_j}\Pi_{i\le j}(1+\frac{Ch_i}{\epsilon\nu_i}),\\
\|D_{x_1}g_j\bar{P}_{j+1}X^{(j)}\|_{\ell_1} &\le \tfrac{C}{h_j\sqrt{\nu_j}},\\
\|\epsilon\widetilde{D}^{(2)}_{x_2}\bar{P}_{j+1}X^{(j)}\|_{\ell_1}+\|h_j\widetilde{D}^{(2)}_{x_1}\bar{P}_{j+1}X^{(j)}\|_{\ell_1} &\le \tfrac{C}{h_j\nu_j}\textstyle\prod_{i\le j}(1+\frac{Ch_i}{\epsilon\nu_i}),\\
\|D_{x_1}\bar{P}_{j+1}X^{(j)}\|_{\ell_1} &\le \tfrac{C}{h_j\sqrt{\nu_j}},
\end{aligned}$$

and by assumption (1.11)

$$\Pi_{i\le j}(1+\frac{Ch_i}{\epsilon\nu_i})\le C.$$

The effect of the post smoothing operator is a consequence of

LEMMA 4.3. *Let*

$$\bar{S}_j=\Pi_{i\le j}S_{i,0}$$

be the post smoothing operator in (2.10), then

$$\bar{S}_jv(x_n)=\sum_{y_{0_k}\in\mathcal{N}_0}\bar{g}_j(y_{0_k})v(x_n-y_{0_k})\quad\forall v\in V_0,\ \ x_n\in\mathcal{N}_0, \tag{4.19}$$

where

$$\bar{g}_j(x_n)\equiv\sum_{y_{i_k}\in\mathcal{N}_i,i=1,\ldots,j}g_0(x_n-y_{1_k})g_1(y_{1_k}-y_{2_k})g_2(y_{2_k}-y_{3_k})\cdot\ldots\cdot g_j(y_{j_k})$$

satisfies

$$\|\bar{g}_j\|_{\ell_1}\le C, \tag{4.20a}$$

$$\|(I-\widetilde{\Pi}_{j+1})\bar{g}_j\|_{\ell_1}\le\frac{Ch_j}{\epsilon\nu_j}. \tag{4.20b}$$

Proof. We have by (4.4)

$$S_{i,0}v(x_n)=\sum_{y_{i_k}\in\mathcal{N}_i}g_i(y_{i_k})v(x_n-y_{i_k}),$$

which implies (4.19); and by (4.6) we see that (4.20a) holds.

Fourier transforming yields

$$\widehat{\bar{g}}_j(\omega)=\Pi_{i\le j}\widehat{g}_i(\omega),$$

ETNA
Kent State University
etna@mcs.kent.edu

where $\widehat{g}_i$ is given in (4.4). Using weighted ℓ_2-norms as in (4.11) we conclude that

$$\begin{aligned} h_{j+1}^2 \|D_{x_1}^{(2)} \bar{g}_j\|_{\ell_1} &\leq \tfrac{C}{\nu_j}, \\ h_{j+1}^2 \|D_{x_2}^{(2)} \bar{g}_j\|_{\ell_1} &\leq \tfrac{C h_j}{\epsilon \nu_j}, \\ h_{j+1}^2 \|D_{x_1} D_{x_2} \bar{g}_j\|_{\ell_1} &\leq \tfrac{C h_j^{1/2}}{\epsilon^{1/2} \nu_j}. \end{aligned}$$

Hence, combining this and the standard estimate of the L_2-projection

$$\|(I - \widetilde{\Pi}_{j+1}) \bar{g}_j\|_{\ell_1} \leq C h_{j+1}^2 \|\bar{g}_j\|_{w_1^2}, \tag{4.21}$$

cf. [13], [10], proves (4.20b). □

5. L_1-estimates of the Green's function in the correction problem. Here we shall estimate the Green's function of the correction problem (4.13), following the idea given in (3.15) and (3.16). Our error representation formula (3.15) is based on the solutions $P_{j+1}\xi_{\nu_j}^{(j)}$ and $\xi_{\nu_j}^{(j)}$ of the correction problem

$$\begin{aligned} h_{j+1}^2 L_{j+1} P_{j+1} \xi_{\nu_j}^{(j)}(x_i) &= a_{j+1}(P_{j+1}\xi_{\nu_j}^{(j)}, \phi_i) \\ &= a_j(\xi_{\nu_j}^{(j)}, \phi_i) = h_{j+1}^2 \bar{P}_{j+1} X^{(j)} \quad \forall \phi_i \in \mathcal{B}_{j+1}, \end{aligned} \tag{5.1}$$

where

$$L_j \xi_{\nu_j}^{(j)} = X^{(j)},$$

and where $X^{(j)}$ is given in (4.3), (4.14), (4.18). The discrete Green's function G_j of the correction problem

$$L_j G_j = \delta, \quad \delta(x_i) \equiv \begin{cases} 0, & 0 \neq x_i \in \mathcal{B}_j, \\ \frac{1}{h_j^2}, & x_i = 0, \end{cases} \tag{5.2}$$

yields the representation

$$\xi_{\nu_j}^{(j)} = G_j * X^{(j)}, \tag{5.3}$$

and by (5.1)

$$P_{j+1}\xi_{\nu_j}^{(j)} = G_{j+1} * \bar{P}_{j+1} X^{(j)}. \tag{5.4}$$

To estimate $(I - \widetilde{\Pi}_j)\xi_{\nu_j, x_1}^{(j)}$, $(I - \widetilde{\Pi}_j) P_{j+1} \xi_{\nu_j, x_1}^{(j)}$, and the other parts of the residual in (3.15) we will use the estimates of $X^{(j)}$ in Lemma 4.2 and the above representations. Therefore, in addition to the estimates of $X^{(j)}$, we need similar estimates of G, which we obtain by Fourier transforming in the x_2-direction. Let the Fourier transform $\widehat{G}$ be defined by

$$\widehat{G}_n(\omega) = h_j \sum_{m \in \boldsymbol{Z}} G(h_j n, h_j m) \exp(i\omega h_j m),$$

$$G(h_j n, h_j m) = (2\pi)^{-1} \int_0^{2\pi/h_j} \widehat{G}_n(\omega) \exp(-i\omega h_j m) d\omega,$$

ETNA
Kent State University
etna@mcs.kent.edu

and extend G to $\boldsymbol{R}^2$ by $G \in V_j$. Then equation (5.2) transforms to

$$\begin{aligned} &\tfrac{1}{6}\widehat{G}_{n-1}[5-\exp(-i\omega h_j)] + \widehat{G}_n[1+\tfrac{\epsilon}{h_j}(1-\cos(\omega h_j)) - \tfrac{i}{3}\sin(\omega h_j)] \\ &+\tfrac{1}{6}\widehat{G}_{n+1}[\exp(i\omega h_j)-1] = \delta_0(n). \end{aligned} \tag{5.5}$$

By z-transforming this difference equation according to $\sum_{n=-\infty}^{\infty} \widehat{G}_n z^n$, we see that its characteristic equation

$$-\alpha_2 z^2 + \alpha_1 z + \alpha_0 = 0$$

has two roots

$$z_\pm = \frac{\alpha_1}{2\alpha_2} \pm \frac{\sqrt{\alpha_1^2 + 4\alpha_2\alpha_0}}{2\alpha_2}, \tag{5.6}$$

where the coefficients satisfy

$$\begin{aligned} \alpha_0 &= \tfrac{1}{6}(\exp(i\omega h_j) - 1), \\ \alpha_1 &= 1 - \tfrac{\epsilon}{h}(1-\cos(\omega h_j)) - \tfrac{i}{3}\sin(\omega h_j), \\ \alpha_2 &= \tfrac{1}{6}(\exp(-i\omega h_j) - 1) + 1. \end{aligned}$$

We shall see that

$$\widehat{G}_n = \begin{cases} a(z_+)^{-n}, & n \geq 0, \\ a(z_-)^{-n}, & n < 0x, \end{cases} \tag{5.7}$$

is the bounded solution of (5.5), where a is given by

$$a = \frac{1}{\alpha_1 - \alpha_2(z_-) - \alpha_0(z_+)}.$$

The function $\widehat{G}_n$ in (5.7) is the bounded solution of (5.5) if $|z_+| \geq 1$ and $|z_-| \leq 1$. We verify these estimates of the characteristic roots in (5.7) by expanding the Taylor series of the function $z_\pm$, given in (5.6), in the variable

$$c' \equiv \frac{\epsilon(1-\cos(\omega h_j))}{h_j},$$

around $c' = 0$, and use that $z_+|_{c'=0} = 1$ to obtain

$$|z_+| \geq 1 + \frac{\epsilon h_j \omega^2}{2} + \mathcal{O}(c'^2) > 1 + c''\epsilon h_j \omega^2, \tag{5.8a}$$

$$|z_+|^{-n/4}|\frac{n}{\sqrt{n\epsilon h_j}}\partial_\omega z_+| \leq C, \quad n \geq 1, \tag{5.8b}$$

$$|z_+|^{-n/4}|\frac{n}{n\epsilon h_j}\partial_\omega^2 z_+| \leq C, \quad n \geq 1, \tag{5.8c}$$

where $|\omega h_j| \leq \pi$, and c'' is a positive constant independent of ϵ and h_j provided $\epsilon/h_j < C < 1$. The estimate (5.8a) implies that

$$|z_-| = \frac{\alpha_0\alpha_2}{|z_+|} \leq \frac{1}{2}. \tag{5.8d}$$

ETNA
Kent State University
etna@mcs.kent.edu

Our next step is to prove

LEMMA 5.1. *There holds for* $A \geq h_j^2/\epsilon$

$$\int_{y_1 \leq A} \int_{-\infty}^{\infty} |G(y_1, y_2)| dy_2 dy_1 \leq CA, \tag{5.9a}$$

$$\int_{A<y_1<B} \int_{-\infty}^{\infty} |D_{x_1} G(y_1, y_2)| dy_2 dy_1 \leq C \log \frac{B}{A}, \tag{5.9b}$$

$$\int_{A<y_1<B} \int_{-\infty}^{\infty} |\epsilon \widetilde{D}_{x_2}^{(2)} G(y_1, y_2)| dy_2 dy_1 \leq C \log \frac{B}{A}, \tag{5.9c}$$

$$\int_{y_1>A} \int_{-\infty}^{\infty} h_j |\widetilde{D}_{x_1}^{(2)} G(y_1, y_2)| dy_2 dy_1 \leq C \frac{h_j}{A}, \tag{5.9d}$$

$$\int_{y_1=A} |G(y_1, y_2)| dy_2 \leq C, \tag{5.9e}$$

$$\int_{y_1=A} |D_{x_1} G(y_1, y_2)| dy_2 \leq \frac{C}{A}. \tag{5.9f}$$

Proof. Let us start to prove (5.9f). We shall use the technique in Lemma 4.1 based on the near and far field decomposition (4.11). Let us first assume that $A \geq h_j^2/\epsilon$, i.e. $y_1 \equiv nh_j \geq h_j^2/\epsilon$, then

$$\begin{aligned} \textstyle\int_{y_1=A} |D_{x_1} G(y_1, y_2)| dy_2 &= \textstyle\int_{|y_2|<\beta_n} |D_{x_1} G(A, y_2)| dy_2 + \int_{|y_2|\geq\beta_n} |D_{x_1} G(A, y_2)| dy_2 \\ &\equiv I + II, \end{aligned}$$

where β_n is chosen as

$$\beta_n = a \begin{cases} \sqrt{\epsilon h_j n}, & n\epsilon \geq h_j, \\ h_j, & n\epsilon < h_j. \end{cases} \tag{5.10}$$

Then by (5.7) and (5.8), we have by the equivalence of ℓ_1 and L_1-norms combined with Parseval's relation

$$\begin{aligned} I &\leq C \|\widehat{D_{x_1} G_n}\|_{L^2} \sqrt{\beta_n} \leq \begin{cases} C/(h_j n), & n \geq 1, \\ C(1/2)^n, & n \leq 0, \end{cases} \\ II &\leq C \left\| (\tfrac{y_2}{\beta_n})^2 D_{x_1} G_n \right\|_{L_2} \sqrt{\textstyle\int_{|y_2|>\beta_n} \frac{dy_2}{(y_2/\beta_n)^2}} \\ &\leq C \left\| (\tfrac{\partial_\omega}{\beta_n})^2 (\widehat{D_{x_1} G_n}) \right\|_{L_2} \sqrt{\beta_n} \leq \begin{cases} C/(h_j n), & n \geq 1, \\ C(1/2)^n, & n \leq 0. \end{cases} \end{aligned}$$

In the last inequality we used

$$|z_+|^{-n/4} |\frac{n\partial_\omega z_+}{\beta_n}|^2 + |z_+|^{-n/4} |\frac{n\partial_\omega^2 z_+}{\beta_n^2}|^2 \leq C,$$

ETNA
Kent State University
etna@mcs.kent.edu

and

$$|\frac{\partial_\omega a}{\beta_n}| + |\frac{\partial_\omega^2 a}{\beta_n^2}| \le C,$$

which both follow from (5.6). Now combining the estimates of I and II above proves that (5.9f) holds. We obtain the estimate (5.9b) by integrating (5.9f). The estimates (5.9c,d,e) follow similarly, using also the relation (4.12′) between $\widetilde{D}_{x_i}^{(2)}$ and $D_{x_i}^{(2)}$. For the case (5.9a), when $y_1 < h_j^2/\epsilon$, the choice of β_n is modified according to (5.10), and we see as above that for $y_1 > 0$, $\int_{\mathbb{R}} |G(y_1, y_2)| dy_2 \le C$, which combined with the exponential decay (5.7) and (5.8a,b,c), for $y_1 < 0$, implies (5.9a). □

6. Estimates of the residual in (3.15). *Proof.* [of Theorem 1.1] In this section we shall combine the results of Sections 4 and 5 to estimate the residual in (3.15), and thereby complete the proof of Theorem 1.1. The residual given by (3.15) has two main parts; the first consists of the projections of $\xi^{(j)} \equiv \xi_{\nu_j}^{(j)}$

$$a_j(\xi^{(j)}, (I - \widetilde{\Pi}_{j+1})\bar{g}_j * \phi), \quad a_{j+1}(P_{j+1}\xi^{(j)}, (I - \widetilde{\Pi}_{j+1})\bar{g}_j * \phi), \tag{6.1}$$

and the second part is the artificial diffusion terms

$$\frac{1}{2}\|(h_0 - h_j)\widetilde{D}_{x_1}^2 \xi^{(j)}\|_{L_1}, \quad \frac{1}{2}\|(h_0 - h_{j+1})\widetilde{D}_{x_1}^2 P_{j+1}\xi^{(j)}\|_{L_1}. \tag{6.2}$$

Both parts will be estimated by the representation (5.3), (5.4)

$$\begin{aligned} \xi^{(j)}(x) &= \sum_{y_n \in \mathcal{N}_j} G_j(y_n) X^{(j)}(x - y_n) h_j^2, \\ P_{j+1}\xi^{(j)}(x) &= \sum_{y_n \in \mathcal{N}_{j+1}} G_{j+1}(y_n) \bar{P}_{j+1} X^{(j)}(x - y_n) h_{j+1}^2, \end{aligned}$$

where $X^{(j)}$, $G_j \in V_j$ and the relevant estimates of X and G are given in Lemmata 4.1-2 and 5.1.

Using that $\sum_l \phi_l = 1$, we have by Lemma 4.3 and (3.15)

$$\begin{aligned} \|L_0 \widetilde{U}_{\text{next}}\|_{\ell_1} &\le \sum_{j=0}^{J-1} \sum_{x_l, x_i \in \mathcal{N}_0} h_0^2 |R(x_i)| \, [\, |a_j(\xi^{(j)}(\cdot\,; x_i), (I - \widetilde{\Pi}_{j+1})\bar{g}_j(-\,\cdot) * \phi_l)| \\ &\quad + |\tfrac{1}{2}(h_0 - h_j)(\widetilde{D}_{x_1}^2 \xi^{(j)}(\cdot\,; x_i), \bar{g}_j(-\,\cdot) * \phi_l)| + \ldots] \\ &\le \|R\|_{\ell_1} \max_i \sum_{j,l} \sum_{y_n \in \mathcal{N}_0} \Big[|(I - \widetilde{\Pi}_{j+1})\bar{g}_j(-y_n) a_j(\xi^{(j)}(\cdot\,; x_i), \phi_{l-n})| \\ &\quad + h_j |\bar{g}_j(-y_n)| \, |(\widetilde{D}_{x_1}^2 \xi^{(j)}(\cdot\,; x_i), \phi_{l-n})| + \ldots \Big] \\ &\le \|R\|_{\ell_1} \max_i \sum_j \Bigg[\|(I - \widetilde{\Pi}_{j+1})\bar{g}_j\|_{\ell_1} \int_{-B}^{B} \int_{\mathbb{R}} |\xi_{x_1}^{(j)}(\cdot\,; x_i)| dx \\ &\quad + \|\bar{g}_j\|_{\ell_1} \int_{\mathbb{R}^2} h_j |\widetilde{D}_{x_1}^{(2)} \xi^{(j)}(\cdot\,; x_i)| dx + \ldots \Bigg] \\ &\le \|R\|_{\ell_1} \max_i \sum_j \Bigg[\frac{C h_j}{\epsilon \nu_j} \int_{-B}^{B} \int_{\mathbb{R}} |D_{x_1} \xi^{(j)}(\cdot\,; x_i)| dx \\ &\quad + \|\bar{g}_j\|_{\ell_1} \int_{\mathbb{R}^2} h_j |\widetilde{D}_{x_1}^{(2)} \xi^{(j)}(\cdot\,; x_i)| dx + \ldots \Bigg], \end{aligned} \tag{6.3}$$

ETNA
Kent State University
etna@mcs.kent.edu

where $+\ldots$ denotes the other similar terms in (3.15). The final step in estimating the L_1-norm of the residual above and in (3.15) is to evaluate the integrals above by applying Lemmata 5.1, 4.2. To take advantage of the favourable x_1-decay of the x_2-integrals of G in (5.9a,d), we sum by parts as follows

$$
\begin{aligned}
\|h_j\widetilde{D}_{x_1}^{(2)}\xi^{(j)}\|_{L_1} \;\leq\; & \left\|\textstyle\sum_{y_1\leq h_j\nu_j^{1/2},\ y\in\mathcal{N}_j} h_j\widetilde{D}_{x_1}^{(2)}X^{(j)}(x-y)G_j(y)h_j^2\right\|_{L_1}\\
& + \left\|\sum_{y_1>h_j\nu_j^{1/2},\ y\in\mathcal{N}_j} h_jX^{(j)}(x-y)D_{x_1}^{(2)}G_j(y)h_j^2\right\|_{L_1}\\
& + \left\|\textstyle\sum_{y_1=h_j\nu_j^{1/2},\ y\in\mathcal{N}_j} h_jX_{x_1}^{(j)}(x-y)G_j(y)h_j\right\|_{L_1}\\
& + \left\|\textstyle\sum_{y_1=h_j\nu_j^{1/2},\ y\in\mathcal{N}_j} h_jX^{(j)}(x-y)G_{j,x_1}(y)h_j\right\|_{L_1}\\
\leq\; & \|h_j\widetilde{D}_{x_1}^{(2)}X^{(j)}\|_{\ell_1}\textstyle\int_{y_1<h_j\nu_j^{1/2}}|G_j(y)|dy\\
& + \|X^{(j)}\|_{\ell_1}\textstyle\int_{y_1>h_j\nu_j^{1/2}}|h_j\widetilde{D}_{x_1}^{(2)}G_j(y)|dy\\
& + \|h_jX_{x_1}^{(j)}\|_{\ell_1}\textstyle\int_{y_1=h_j\nu_j^{1/2}}|G_j(y)|dy_2\\
& + \|h_jX^{(j)}\|_{\ell_1}\textstyle\int_{y_1=h_j\nu_j^{1/2}}|G_{j,x_1}(y)|dy_2 \leq \frac{C}{\nu_j^{1/2}}.
\end{aligned}
\tag{6.4}
$$

The other part $h_j\widetilde{D}_{x_1}^{(2)}P_{j+1}\xi^{(j)}$ in (6.3) can be estimated similarly and satisfies the same bound. We note that by assumption (1.11) $\nu_j^{1/2}\gg h_j/\epsilon$, which implies that $A=h_j\nu_j^{1/2}\gg h_j^2/\epsilon$, and therefore the assumption in Lemma 5.1 holds. By choosing $A=Ch_j$ in Lemma 5.1, it follows similarly that

$$
\int_{-B}^{B}\int_{\mathbb{R}}|\xi_{x_1}^{(j)}|dx+\int_{-B}^{B}\int_{\mathbb{R}}|\epsilon\widetilde{D}_{x_2}^{(2)}\xi^{(j)}|dx\leq C\log\frac{B}{h_j}.
\tag{6.5}
$$

Combining (6.3-5) proves Theorem 1.1. □

Remark. In the particular case studied here, the Green's functions g and G in (4.4) and (5.2), respectively, are translation invariant, and hence also $\xi^{(j)}$ becomes translation invariant, i.e. $\xi^{(j)}(x;x_n)=\xi^{(j)}(x_n;x)=\kappa(x-x_n)$ for a certain function κ. Therefore, the sum over x_i in (3.15) is in fact a convolution and hence, by the Youngs inequality, the ℓ_1-norm in Theorem 1.1 can be replaced by any L_p-norm, $1\leq p\leq\infty$.

7. Numerical results and extensions. In this section we discuss some extensions of Theorem 1.1 and numerical experiments of the multigrid method. The extensions are motivated by the continuous analogue of the multigrid method in (3.16-24) and by numerical experimentsf; a rigorous analysis of the discrete case following Theorem 1.1 is tedious and is not carried out here.

7.1. Non-aligned mesh. Assume that we solve the equation

$$
u_{x_1}+\frac{1}{2}u_{x_2}-\epsilon\Delta u=f
$$

with the streamline diffusion finite element method using the mesh in Fig. 2, Section 4. Then, the characteristic direction $(1,1/2)$ is not parallel to any edge of the mesh and the difference

ETNA
Kent State University
etna@mcs.kent.edu

operator corresponding to (4.2) takes the form

$$
\begin{aligned}
&(L_j X^{(j)})(h_j n, h_j m) = \tfrac{1}{h_j}[X^{(j)}(h_j n, h_j m) - \tfrac{1}{2}X^{(j)}(h_j(n-1), h_j m) \\
&+\tfrac{1}{8}X^{(j)}(h_j n, h_j(m-1)) - \tfrac{1}{2}X^{(j)}(h_j(n-1), h_j(m-1)) + \tfrac{1}{8}X^{(j)}(h_j n, h_j(m+1))] \\
&+\tfrac{\epsilon}{h_j^2}[-\tfrac{1}{4}X^{(j)}(h_j n, h_j(m+1)) + \tfrac{1}{2}X^{(j)}(h_j n, h_j m) - \tfrac{1}{4}X^{(j)}(h_j n, h_j(m-1))].
\end{aligned} \tag{7.1}
$$

In orthogonal coordinates (ζ_1, ζ_2), with ζ_1 aligned with the characteristic $(1, 1/2)$, the Fourier transform of L_j has fourth order dissipation in the ζ_2-direction in contrast to the operator in (4.2). The L_1-norm of the Green's function for the post smoothing operator, cf. (3.16), related to the continuous version of L_j

$$\frac{\partial}{\partial \zeta_1} - \epsilon\Delta - \frac{2h_j^3}{625}\frac{\partial^4}{\partial \zeta_2^4},$$

can be estimated by $\|(I - \widetilde{\Pi}_{j+1})\bar{g}_j\|_{L_1} \leq \frac{Ch_j^2}{\sqrt{\frac{2}{625}h_j^4\nu_j + h_j\epsilon\nu_j}}$ replacing $\frac{Ch_j^2}{h_j\epsilon\nu_j}$ in (1.10). The artificial diffusion term in (1.10), i.e. the $C_2/\sqrt{\nu}_j$ term, does not change. This replacement indicates that the multigrid method, based on Jacobi smoothing steps, could work for $\epsilon = 0$ and $h_0 > 0$ if the mesh is not aligned with the characteristic; however, due to the small factor 2/625, the number of smoothing steps required to sufficiently damp one V-cycle might be very large. After one V-cycle, Experiment B in Table 1 shows large amplifications of 5.4 and 4.7 for five and ten smoothing steps, respectively. However, after several cycles the asymptotic damping is strictly less than 1.0 using five and ten smoothing steps. This is in contrast to the aligned case of experiment G, in the same table, where the damping degenerates to 1.0 as ϵ/h_0 tends to zero. Hence, an analysis of the asymptotic damping, for $\epsilon/h_0 \ll 1$, in the non-aligned case would require a study of the residual in multiple cycles, cf. Section 7.2.

7.2. Isotropic artificial diffusion and the effect of several V-cycles. As mentioned in Section 1, to stabilize the convection problem we can also use the first order accurate isotropic artificial diffusion $(h_j\nabla U, \nabla v)$ instead of the streamline diffusion form $(h_j U_{x_1}, v_{x_1})$. The isotropic form gives an additional artificial diffusion term $(h_0 - h_j)\widetilde{D}_{x_2}^{(2)}\xi^{(j)}$ in (3.11), (3.15), which has the same estimate as $\epsilon D_{x_2}^{(2)}\xi^{(j)}$ in (6.5) and yields the additional contribution

$$\int_{-B}^{B}\int_{\mathbb{R}} |(h_0 - h_j)\widetilde{D}_{x_2}^{(2)}\xi^{(j)}|dx \leq C\log\frac{B}{h_j}$$

to the corresponding γ_B in (1.10). Also in practice, one V-cycle based on isotropic diffusion and post smoothing, does not damp the residual for fine meshes, cf. experiments D,E,F in Table 1, and the damping factor is increasing with larger domains. However, several cycles damp the residual. Let us briefly try to explain this behavior of the damping for the two grid method with $h_1 = 2h_0$. The evolution of the initial Dirac measure residual yields, after one V-cycle, a small part R_2 of the residual error with L_1-norm

$$\|R_2\|_{L_1} \leq \frac{C_1}{\nu_0}\log\frac{B}{h_0} + \frac{C_2}{\sqrt{\nu}_0},$$

and a larger part R_1 which is the artificial diffusion term $(h_1 - h_0)\widetilde{D}_{x_2}^{(2)}P_1\xi^{(1)}$. Let us now study the evolution of the x_2-Fourier transform of the residual error, caused by the artificial x_2-diffusion,

$$R_1 \equiv \theta(x_1)\frac{h_1}{2}\omega^2\exp(-\omega^2 x_1 h_1), \quad \theta(x_1) \equiv \begin{cases} 1, & x_1 > 0, \\ 0, & x_1 \leq 0. \end{cases}$$

ETNA
Kent State University
etna@mcs.kent.edu

TABLE 1.

Experiment	ϵ	method	h_{fine}	h_{coarse}	ν_{pre}	ν_{post}	$\gamma(1)$	$\gamma(5)$	$\bar{\gamma}$
A	1/64	SD	1/64	1/4	3	3	1.87	0.113	0.495
A	1/64	SD	1/64	1/4	5	5	1.25	0.0230	0.368
A	1/64	SD	1/64	1/4	10	10	0.647	0.00178	0.229
B	0	SD,α	1/64	1/4	5	5	5.39	-	0.880
B	0	SD,α	1/64	1/4	10	10	4.69	-	0.777
C	1/64	SD	1/64	1/4	3	0	4.74	0.760	0.633
C	1/64	SD	1/64	1/4	5	0	4.22	0.308	0.520
C	1/64	SD	1/64	1/4	10	0	3.59	0.0525	0.348
D	h_j	ISO	1/8	1/4	5	5	0.676	0.0174	0.400
D	h_j	ISO	1/16	1/8	5	5	0.907	0.0446	0.471
D	h_j	ISO	1/32	1/16	5	5	1.14	0.0708	0.499
D	h_j	ISO	1/64	1/32	5	5	1.35	0.0961	0.516
E	h_j	ISO	1/8	1/4	5	5	0.676	0.0174	0.400
E	h_j	ISO	1/16	1/4	5	5	1.08	0.0902	0.537
E	h_j	ISO	1/32	1/4	5	5	1.53	0.245	0.633
E	h_j	ISO	1/64	1/4	5	5	2.00	0.502l	0.707
E	h_j	ISO	1/128	1/4	5	5	2.53	0.915	0.775
F	h_j	ISO	1/8	1/4	10	10	0.482	0.00205	0.256
F	h_j	ISO	1/16	1/4	10	10	0.840	0.0159	0.371
F	h_j	ISO	1/32	1/4	10	10	1.24	0.0555	0.460
F	h_j	ISO	1/64	1/4	10	10	1.71	0.166	0.558
F	h_j	ISO	1/128	1/4	10	10	2.20	0.379	0.644
G	$1/32$	SD	1/64	1/4	5	5	1.20	-	0.362
G	$1/128$	SD	1/64	1/4	5	5	1.37	-	0.438
G	$1/512$	SD	1/64	1/4	5	5	2.05	-	0.606
G	$1/2048$	SD	1/64	1/4	5	5	3.45l	-	0.784
G	$1/8192$	SD	1/64	1/4	5	5	4.17	-	0.885
G	$1/32768$	SD	1/64	1/4	5	5	4.40	-	0.922
G	0	SD	1/64	1/4	5	5	4.48	-	~ 1

Residual damping ratio of multigrid V-cycles. We use multigrid iterations to solve $u_{x_1} - \epsilon\Delta u = 0$ in $(0,1) \times (0,1)$, with an initial Dirac-like algebraic residual with L_1-norm 1.0 at the center of the computational domain. We use the homogeneous Dirichlet boundary conditions except at the outflow boundary at $x_1 = 1$, where the homogeneous Neumann boundary condition is applied. The constant in the damped Jacobi steps is $c = 0.2$. The number of pre and post smoothing steps are increased by a factor of two on each coarser level, i.e. $\nu^j_{pre} = 2^j \nu_{pre}$. The L_1-norm of the residual after n V-cycles is $\gamma(n)$, and $\bar{\gamma} \equiv (\gamma(5)/\gamma(1))^{1/(5-1)}$ the average damping of V-cycles 2 to 5, which in practice approximates the asymptotic damping of one V-cycle, except in experiment B and G where the 5 in $\bar{\gamma}$ is changed to 15. Note that $\gamma(0) = 1.0$. In experiment B, the convective part u_{x_1} has been replaced by $\nabla u \cdot (\cos\alpha, \sin\alpha)$, where α is the angle to the x_1-axis. In experiment B, we choose $\tan\alpha = 1/4$, i.e the characteristic is not aligned with the mesh. In the last experiment of G, with $\epsilon = 0$, the residual is not asymptotically damped.

ETNA
Kent State University
etna@mcs.kent.edu

Initially in the second V-cycle, the Fourier transformed iteration error ξ_2, due to artificial diffusion, satisfies

$$\xi_{2,x_1} + h_0\omega^2\xi_{2,x_2x_2} = R_1,$$

and then in the smoothing steps (which is multiplication by $\exp(-\omega^2 h_0^2\nu_0)$ for the x_2-part) this residual remains approximately the same (for $|x_1|$ not too small). Therefore, its correction condition

$$P_1\xi_{2,x_1} + h_1\omega^2 P_1\xi_2 = R_1,$$

with the solution

$$P_1\xi_2 = \theta(x_1)\frac{h_1}{2}\omega^2 x_1 \exp(-\omega^2 x_1 h_1),$$

describe the residual error

$$\frac{h_1}{2}\omega^2 P_1\xi_2 = \frac{\theta(x_1)}{x_1}(\frac{h_1 x_1\omega^2}{2})^2 \exp(-\omega^2 x_1 h_1).$$

Combining the residual error in the last equation, the smaller error R_2, and making a slight modification in $P_1\xi_2$ for $|x_1| \le Ch_0$ (due to damping in the smoothing), we obtain the following residual damping after n cycles

$$\gamma_B = (G(n) + \frac{C_1}{\nu_0})\log\frac{B}{h_0} + \frac{C_2}{\sqrt{\nu}_0},$$

where

$$G(n) \equiv \int_{I\!R} |\mathcal{F}^{-1}(\frac{h_1 x_1\omega^2}{2})^n \exp(-\omega^2 h_1 x_1)| dx_2.$$

The operator $\mathcal{F}^{-1}$ denotes the inverse Fourier transform in the x_2-direction. A numerical computation shows that $G(4) = 0.02346$ is the minimum of G; other values of G are $G(0) = 1$, $G(1) = 0.121$, $G(3) = 0.0270$ and $G(5) = 0.0263$. Hence in the two grid method the residual will be damped after four V-cycles provided $B/h_0 < 10^{18}$ and ν_0 is chosen such that $\|R_2\|_{L_1} \le 1/2$. Experiments D,E,F in Table 1 show that a residual, which has an initial L_1-norm of size 1.0, may increase after one iteration, but after some additional V-cycles the residual is damped below its initial value.

7.3. Higher dimensions. In d dimensions the problem (1.1) and the estimates corresponding to the residual X in (3.14) and the Green's function ξ in (3.16) are changed by replacing x_2^2 by $\sum_{i=2}^d x_i^2$ in the exponential and the appropriate square root in the denominator by $(\cdot)^{d-1/2}$. This change does not alter the estimates (3.17-19). Therefore, we expect the estimate (1.10) of γ_B to hold in d dimensions, $d > 2$.

7.4. Higher order elements. For kth order elements we have two choices. Either we can, (i) use the higher order method also on coarser levels, or we can, (ii) compute the correction with piecewise linear elements on *the same mesh/* and on all coarser meshes. For $k = 2$, iterations based on (i) and (ii) use the same number of degrees of freedom. Both strategies work numerically. In alternative (i), we can use in (3.23)

$$\|(I - \widetilde{\Pi}_{j+1})\bar{g}_j\|_{L_1} \le C_k h_{j+1}^{k+1}\|\bar{g}_j\|_{W_1^{k+1}}, \tag{7.2}$$

ETNA
Kent State University
etna@mcs.kent.edu

which for case (i) has the bound

$$C_k(\frac{2h_j}{\sqrt{h_j\epsilon\nu_j}})^{k+1} = C_k 2^{k+1}(\frac{h_j}{\epsilon\nu_j})^{(k+1)/2}$$

instead of

$$C_1\frac{(2h_j)^2}{h_j\epsilon\nu_j} = C_1 4\frac{h_j}{\epsilon\nu_j}$$

in (3.24). The case (ii) similarly yields the bound

$$C_1\frac{h_j^2}{h_j\epsilon\nu_j} = C_1\frac{h_j}{\epsilon\nu_j}.$$

Hence, considering $h_j/(\epsilon\nu_j)$ close to 1, the piecewise linear case (ii) gives a damping which is a factor $2^{-(k+1)}C_1/C_k$ smaller than the damping in case (i), indicating that the alternative (ii) is more efficient. The constant $C_k \sim 1/(k+1)$ is the interpolation constant in (7.2). The computational cost for one V-cycle using alternative (ii) is also lower than for case (i), since the assembled matrix is sparser for linear elements and a lower order quadrature rule is required. In practice it is possible for many problems to use streamline diffusion (for quadratic elements) on the finest level $j = 0$ and first order isotropic artificial diffusion on the correction problems with piecewise linear elements on levels $j = 1, 2, \ldots, J$. This scheme combines the higher order approximation of the streamline diffusion method with the robust and cheap smoothing on the correction problems and is used in the computation shown in Fig. 6 in Section 8.3.

7.5. Estimates of the error. The multigrid method needs a criteria on how small the residual $a(U,\cdot) - (F,\cdot)$ should be to terminate the V-cycle iterations. Becker, Johnson and Rannacher [4] have studied such criteria determined by *a posteriori* estimates and the requirement that: (i) the discretization error from the finite element method, and (ii) the error caused by solving the equations approximately by the multigrid method, are of the same order. The multigrid error e_M of (ii) can be written, (see [4], [20]),

$$e_M(y) = \int_{\mathbb{R}^2} R\psi dx, \tag{7.3}$$

where $R \sim U_{x_1} - \epsilon\Delta U - F$ is the residual and ψ solves the continuous problem, dual to (1.1),

$$\begin{aligned} L^*\psi \equiv -\psi_{x_1} - \epsilon\Delta\psi &= \delta(\cdot - y), \text{ in } \Omega, \\ \psi|_{\partial\Omega} &= 0. \end{aligned}$$

Therefore, ψ is the dual function of the Green's function ξ in (3.16), and satisfies the same estimate (3.20), with x replaced by $(-(x_1 - y_1), x_2 - y_2)$. This estimate and (7.3) imply

$$|e_M(y)| \le \frac{C\|R\|_{L_1}}{\sqrt{h_j\epsilon}},$$

and since $\|R\|_{L_1}$ is damped, the error e_M can be made arbitrary small by increasing the number of V-cycles. If the correction problems have consistent bilinear forms, then the orthogonality in the correction problems can be used to improve the estimate (7.3), see [4]. In our case the similar procedure would be to base an *a posteriori* estimate on (3.9) or (3.15).

ETNA
Kent State University
etna@mcs.kent.edu

7.6. A singular perturbed symmetric elliptic problem. Consider for $\epsilon \ll 1$ the singular perturbed symmetric elliptic problem

$$\begin{aligned} u_{x_1x_1} + \epsilon u_{x_2x_2} &= f, \quad x \in \Omega, \\ u|_{\partial\Omega} &= 0. \end{aligned} \tag{7.4}$$

The damping in the V-cycle can be analyzed analogously, to the problem (1.1), with the difference that the artificial diffusion terms in (3.15) now are absent and the post smoothing operator $\bar{g}_j$ satisfies

$$\|(I - \widetilde{\Pi}_{j+1})\bar{g}_j\|_{L_1} \leq \frac{C}{\epsilon\nu_j},$$

since the Gaussian in (3.14) changes to

$$X(x,t) = \frac{\exp[-x_1^2/(4cth_j^2) - x_2^2/(4cth_j^2\epsilon)]}{4\pi tch_j^2\epsilon^{1/2}}.$$

The L_1-norm of the residual has the same estimate as in (3.22)

$$\int_{-B}^{B}\int_{\mathbb{R}} (|\xi_{x_1x_1}| + \epsilon|\xi_{x_2x_2}|)dx \leq C\log\frac{B}{h_j},$$

and we conclude that the damping satisfies

$$\gamma_B \leq \sum_{j=0}^{J-1} \frac{C}{\epsilon\nu_j}\log\frac{B}{h_j}.$$

Compared to the damping (1.10) for the convective problem (1.1), the above damping is larger by a factor $1/h_j$. Indeed, numerical experiments indicate that the convergence of the multigrid method for (7.4) is slower than for problem (1.1).

7.7. Small and large diffusion. In Fig. 3 we compare by numerical experiments the residual of the convection diffusion equation (1.1) for $\epsilon = h_0$ and $\epsilon = 1$. We see that the damping yields residuals which in both cases are qualitatively the same.

In agreement with the analysis of Theorems 1.1 and 1.2, numerical experiments show that the L_1-norm of the V-cycle residuals due to an initial Dirac residual function (3.3) is larger than the residuals due to other initial functions (with the same L_1-norm).

For a fixed number of pre and post smoothing steps the L_1-norm of the residual after one V-cycle in Theorem 1.1 is bounded by $\tilde{C}_1 + \tilde{C}_2/\epsilon$. Experiment G in Table 1 shows that this is a good estimate for $\epsilon/h_0 \geq 1/32$. For the case $\epsilon \ll h_0$, the L_1-norm of the residual after one V-cycle is uniformly bounded; but the experiments also show that the asymptotic residual quotient, in two consecutive V-cycles, becomes arbitrary close to 1, and hence the multigrid method does not work; see Section 7.1.

ETNA
Kent State University
etna@mcs.kent.edu

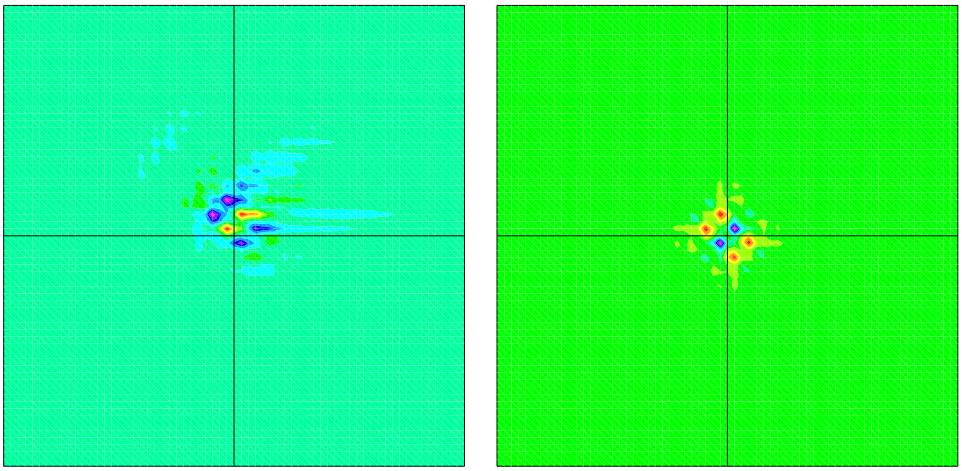

FIG. 3. *Spatial distribution of the residuals for the convection-diffusion problem of Table 1. The convection is in the x_1-direction. Two choices of the diffusion ϵ are studied: To the left, $\epsilon = h_0 = 1/64$ with streamline diffusion stabilization, and to the right, $\epsilon = 1$. The initial residual is a Dirac function with L_1-norm 1.0 at the center of the computational domain. For both sizes of diffusion we use V-cycle iterations with $\nu^j_{pre} = \nu^j_{post} = 5 \cdot 2^j$ damped Jacobi smoothing steps, with finest level $j = 0$, $h_0 = 1/64$, and coarsest level $j = 4$ with $h_4 = 1/4$. After five V-cycle iterations the L_1-norm of the algebraic residual has been damped from 1.0 to 0.023 and 0.0084, for the small and large diffusion case, respectively. We conclude from the figures above that in both cases the residual damping is caused by diffusion and not by transport.*

7.8. No post smoothing. The projection part of the residual in (3.11), for a V-cycle without post smoothing, will be damped by the pre smoothing steps on the appropriate level in the next V-cycle

$$S_{j,0}P_jS_{j-1,0}P_{j-1}\dots P_2S_{1,0}P_1S_{0,0}(I-\widetilde{\Pi}_j)\widetilde{L}_j\xi^{(j)},$$

which is similar to the smoothing by $\bar{g}_j$ in a post smoothing step, cf. (3.13). Therefore, we expect the damping for two V-cycles without post smoothing to be close to the damping of one V-cycle with post smoothing. This is confirmed in Table 1, experiments A,C.

7.9. Distribution of smoothing steps and Navier-Stokes equations. What is the optimal distribution of smoothing steps on the different levels in a multigrid method? For pure diffusion problems the optimal strategy is to use the same number of smoothing steps, ν_j, on every level, j; see [16]. Here we compare this strategy $\nu_j = \nu_{01} = constant$, with the alternative $\nu_j = \nu_{02}\ 2^j = constant\ 2^j$, where the number of smoothing steps increase exponentially on coarser meshes. By choosing $\nu_{01} = 15$ and $\nu_{02} = 10$ the two strategies give the same amount of work, for a uniform mesh where each triangle is refined into four new triangles. The numerical results in Fig. 4 show that the $\nu_j = 10 \cdot 2^j$-strategy is the best of these two smoothing strategies, when they are applied to the stationary two-dimensional compressible Navier-Stokes equations for an ideal gas with specific heat ratio γ, (see [21]), artificial viscosity, $\epsilon = 0.01$, and source term, f,

$$\text{div}\, F(W) = \epsilon\Delta W + f, \tag{7.5}$$

ETNA
Kent State University
etna@mcs.kent.edu

where $W = (\rho, \rho u, \rho v, \rho E)$ is the vector consisting of the density, momentum in the x_1 and x_2 directions and the energy.

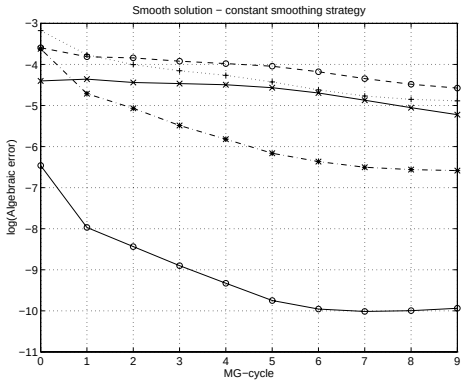

FIG. 4A

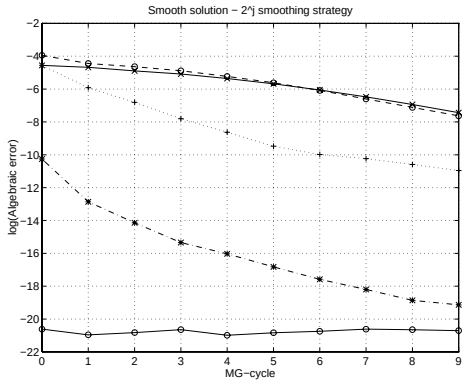

FIG. 4B

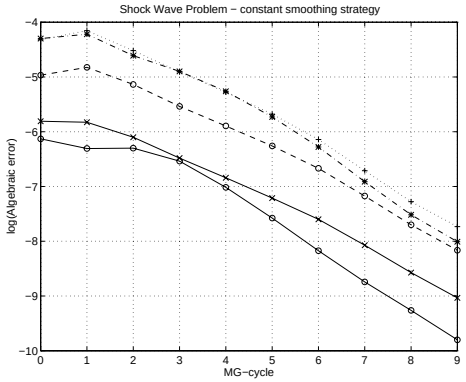

FIG. 4C

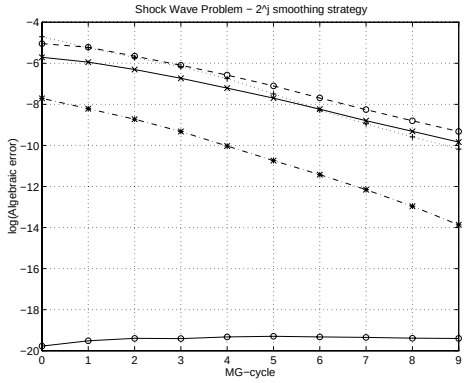

FIG. 4D

FIG. 4. *Algebraic residual for a smooth solution and a shock wave solution of the Navier-Stokes equations in Section 7.9, using the nonlinear full approximation multigrid scheme with damped Jacobi smoothing steps. The graphs show the algebraic residual error for the finest level and its correction problems on coarser levels. The graphs compare the algebraic residual error with six levels of multigrid cycles using* $\nu_j = 15$ *and* $\nu_j = 10 \cdot 2^j$*, respectively, number of smoothing steps on level* j*. These two strategies have the same amount of work. The finest level,* $j = 0$*, has* 3969 *nodal points for the problem with the smooth solution, and* 15041 *nodal points for the shock problem. Fig. 4AB and Fig. 4CD show the residual error for the smooth solution (7.5-6), and the shock wave problem (7.5),(7.7), respectively. The algebraic residual error is marked as follows. Finest level* $j = 0$ *: solid line with crosses, level* $j = 1$ *: dashed line with circles, level* $j = 2$ *: dotted line with plus, level* $j = 3$ *: dash-dotted line with stars and level* $j = 4$ *: solid line with circles. We note that the residual on the finest level is smaller for the* $\nu_j = 10 \cdot 2^j$ *strategy, and therefore this strategy is better. Moreover, the residual errors for the correction problems on level* $j = 1$ *and* $j = 2$ *are larger for the strategy* $\nu_j = 15$*, indicating that they should be solved more accurately.*

ETNA
Kent State University
etna@mcs.kent.edu

To prevent oscillations on coarser grids, we add a numerical artificial diffusion term, $(\sqrt{\epsilon^2 + (h\beta)^2} - \epsilon)\Delta W$, where β denotes the maximal absolute value of the eigenvalues of the two Jacobians defined by the flux F, and h denotes the mesh size. The finest level problem and the coarser problems are solved with piecewise linear elements using this isotropic artificial diffusion and the non-linear full approximation multigrid method with damped Jacobi smoothing steps; see [7] and Section 8. The mesh refinement is global and uniform. We study two problems. The first problem has a smooth solution and the second problem has a planar stationary shock. In the case of the smooth solution, $\gamma = 1.4$ and the source term f is chosen to satisfy (7.5) for the solution

$$(\rho, u, v, E) = (1 + \frac{1}{2}(x_1^2 + x_2^2))(1, 1, 1, 1), \tag{7.6}$$

and the computation is performed on the unit square. The shock wave problem is solved with $f = 0,\ \gamma = 2.0$ and the boundary conditions

$$\begin{aligned} W(0, x_2) &= (1, \sqrt{3.5}, 0, 2.75), \\ W(4, x_2) &= (1.4, \sqrt{3.5}, 0, 3.25), \end{aligned} \tag{7.7}$$

in the computational domain $(0, 4) \times (0, 1)$. The computations in Fig. 4 show that the $\nu_j = 10 \cdot 2^j$-strategy yields a smaller residual than by choosing the smoothing steps as $\nu_j = 15$. Numerical experiments also show that the $\nu_j = 2^j \nu_{02}$-strategy is more robust than the $\nu_j = \nu_{01}$-strategy, when decreasing the constants ν_{0i} in an equi-work consistent way. When ν_{01} is chosen below 10 the method becomes unstable.

8. A 2D shock wave problem. The two-dimensional nonlinear shock wave problem

$$\begin{aligned} F(u) \equiv (\tfrac{u^2}{2})_{x_1} - \epsilon\Delta u &= 0, \quad x = (x_1, x_2) \in \boldsymbol{R}^2, \\ u(\pm\infty, \cdot) &= \mp 1, \end{aligned} \tag{8.1}$$

has a stationary one-dimensional Burgers shock solution, and it can be solved by the full multigrid method based on the full approximation scheme (see [7]); the smoothing operator $S_{0,0}$ is then given by (2.2) and (3.16) with $F(u)$ replacing Lu and the correction step is

$$U_{\text{next}}^{\text{pre}} = S_{0,0}U_0 - (\bar{U} - \pi_1 S_{0,0}U_0).$$

Here, the mesh size is chosen such that $h_0 \sim \epsilon$, the operator π_1 is the nodal interpolant onto V_1, and $\bar{U} \in \{v : v|_K \in \mathcal{P}_1(K)\ \forall K \in T^{h_1}\}$ satisfies

$$F_{h_1}(\bar{U}, v) = F_{h_1}(\pi_1 S_{0,0}U_0, v) + F_\epsilon(S_{0,0}U_0, v) \quad \forall v \in V_1,$$

and

$$F_h(u, v) \equiv \int_{\boldsymbol{R}^2} [(\frac{u^2}{2})_{x_1} v + h\nabla u \nabla v] dx.$$

When the perturbations $w = U_{\text{next}}^{\text{pre}} - U_0$ become sufficiently small, the nonlinear two grid method above is approximated by the two level method (1.6) for the linearized problem

$$\mathcal{L}w \equiv (u(x_1)w)_{x_1} - \epsilon\Delta w = 0, \tag{8.2}$$

which is a convection-diffusion problem where the compressive flow $u(x_1) = -\tanh\frac{x_1}{2\epsilon}$ is a Burgers shock wave solving (8.1). We have chosen the coordinates so that $x_1 = 0$ is the center of the wave.

ETNA
Kent State University
etna@mcs.kent.edu

We study the damping of the two grid method for (8.2), where for simplicity $h_0 = \epsilon$ and $h_1 = 2h_0$. To begin, we need a representation of the residual. The residual representation (3.15) for the constant coefficient problem (1.1) used translation invariance of the post smoothing operator $\bar{g}_j$; for the shock wave problem (8.2) the corresponding smoothing operator is not translation invariant due to the x_1-dependent flow $u(x_1)$. Our first step is to derive a residual representation, in view of the related continuous problem, described in (3.16-24). Now the orthogonality of the correction problem for post smoothing is based on the property that $\mathcal{L}$ and $S_{0,0}$ commute, which is proved in Lemma 8.1 below. The second step is to study the Green's function for (8.2) and estimate the damping of the two grid method.

8.1. Residual representation. The Green's function $g(x,t;\underline{x},\underline{t})$ for the shock wave equation (8.2)

$$\begin{aligned} g_t + h_0\mathcal{L}g &= 0, \quad t > \underline{t}, \\ g(x,\underline{t};\underline{x},\underline{t}) &= \delta(x-\underline{x}), \end{aligned} \tag{8.3}$$

and its dual

$$\psi(x,t;\bar{x},\bar{t}) = g(\bar{x},\bar{t};x,t), \tag{8.4}$$

$$\begin{aligned} -\psi_t + h_0\mathcal{L}^*\psi \equiv -\psi_t + h_0[-u(x_1)\psi_{x_1} - \epsilon\Delta\psi] &= 0, \quad t < \bar{t}, \\ \psi(x,\bar{t};\bar{x},\bar{t}) &= \delta(x-\bar{x}), \end{aligned} \tag{8.5}$$

are both translation invariant in time, but not in space since $u = u(x_1)$.

Let the smoothing operator S be defined by

$$Sv(x) = \int_{\boldsymbol{R}^2} g(x,\nu;y,0)v(y)dy, \tag{8.6}$$

then we have

LEMMA 8.1. *The operators $\mathcal{L}$ and S commute.*

Proof. We have by (8.3-6)

$$\begin{aligned} S\mathcal{L}v &= \textstyle\int_{\boldsymbol{R}^2} g(x,\nu;y,0)\mathcal{L}v(y)dy = \int_{\boldsymbol{R}^2} \mathcal{L}_y^* g(x,\nu;y,0)v(y)dy \\ &= \textstyle\int_{\boldsymbol{R}^2} \mathcal{L}_y^*\psi(y,0;x,\nu)v(y)dy = \int_{\boldsymbol{R}^2} h_0^{-1}\psi_t(y,0;x,\nu)v(y)dy \\ &= -\textstyle\int_{\boldsymbol{R}^2} h_0^{-1} g_t(x,\nu;y,0)v(y)dy = \int_{\boldsymbol{R}^2} \mathcal{L}_x g(x,\nu;y,0)v(y)dy = \mathcal{L}Sv, \end{aligned}$$

where the subscript of operator $\mathcal{L}$ (and K, Δ below) denotes the dependent variable. ∎

Let the evolution of the Green's function for the two grid iteration error be defined by, cf. (3.4), (3.16),

$$\begin{aligned} \xi_t + h_0\mathcal{L}\xi &= 0, \quad t > 0, \\ \mathcal{L}\xi(x,0) &= \delta(x-\bar{x}). \end{aligned}$$

A small modification in the treatment of the correction problem (3.9), yields as in (3.11) the residual error

$$\begin{aligned} \mathcal{L}_0(\widetilde{U}_{\text{next}}^{\text{pre}})(x_l) &= \sum_{x_i\in\mathcal{N}_0} [(\widetilde{\mathcal{L}}_0\xi_{\nu_0}^{(0)}, \phi_l - r) - (\widetilde{\mathcal{L}}_0 P_1\xi_{\nu_0,x_1}^{(0)}, \phi_l - r) \\ &\qquad - (h_0 - h_1)(\Delta P_1\xi_{\nu_0}^{(0)}, r)]R(x_i) \quad \forall r \in V_1, \end{aligned} \tag{8.7}$$

ETNA
Kent State University
etna@mcs.kent.edu

where P_1 is defined as in (2.4) for the bilinear form corresponding to the problem (8.2). Given ϕ_l, choose now r according to

$$r = \frac{\int_{\boldsymbol{R}^2} \phi_l(x)dx}{\int_{\boldsymbol{R}^2} \sum_{\bar\phi_k \in \mathcal{B}_{1,l}} \bar\phi_k(x)dx} \sum_{\bar\phi_n \in \mathcal{B}_{1,l}} \bar\phi_n, \tag{8.8}$$

where $\mathcal{B}_{1,l} \equiv \{\bar\phi_n \in \mathcal{B}_1 : x_n \in \text{supp}(\phi_l)\}$, $\text{supp}(\phi_l) \equiv \overline{\{x : \phi_l(x) \neq 0\}}$ and expand r in the basis $\mathcal{B}_0$

$$r(x) = \sum_{x_i \in \mathcal{N}_0,\ \phi_i \in \mathcal{B}_0} r(x_i)\phi_i(x).$$

Then, we have

$$(\widetilde{\mathcal{L}}_0\xi, \phi_l - r) = (\widetilde{\mathcal{L}}_0\xi, \phi_l) - \sum_{x_i \in \mathcal{N}_0} (\widetilde{\mathcal{L}}_0\xi, \phi_i) r(x_i) \equiv (K(\widetilde{\mathcal{L}}_0\xi, \phi_\cdot))_l, \tag{8.9}$$

where the difference operator K satisfies

$$\begin{aligned} K_{ij} &= 0, \quad |x_i - x_j| > \sqrt{2}h_0, \\ Kp &= 0 \quad \forall p \in \{\text{polynomials of degree at most } 1\}, \end{aligned}$$

and K is a difference operator of second order. This, and interpolation estimates like (4.21) imply that

$$\|KX\|_{\ell_1} \leq C\|h_0^2 X\|_{w_1^2}. \tag{8.10}$$

By Lemma 8.1 and (8.7) we obtain the following representation for the residual

$$\begin{aligned} |\mathcal{R}| &\equiv |\mathcal{L}S(\xi - P_1\xi)| = |S\mathcal{L}(\xi - P_1\xi)| \\ &\leq |SK\mathcal{L}\xi| + |SK(\mathcal{L} - (h_1 - h_0)\Delta)P_1\xi| + |(h_0 - h_1)S\Delta P_1\xi|. \end{aligned} \tag{8.11}$$

The same steps carry over directly to the discrete version of the operator $\mathcal{L}$ and smoothing S in the two level method.

8.2. Damping by smoothing. To estimate the L_1-norm of the residual $\mathcal{R}$ in (8.11) we need an estimate of the smoothing operator S and the function ξ. The residual

$$X \equiv (u(x_1)\xi)_{x_1} - h_0\Delta\xi = \mathcal{L}\xi$$

satisfies the same equations as the iteration error ξ

$$X_t + h_0\mathcal{L}X = 0, \tag{8.12}$$

since the operator $\mathcal{L}$ is time independent. We shall now study the Green's function $X(\cdot, t) = g(\cdot, t; \bar{x}, 0)$ with $X(\cdot, 0) = \delta(\cdot - \mathrm{x})$ for x in the shock wave region $B \equiv \{(x_1, x_2) \in \boldsymbol{R}^2 : |x_1| \leq Ch_0\}$. The other case when the residual is far away from the shock, i.e. when x is far from the shock, is for the first V-cycles related to the constant coefficient problem (1.2). In Section 7.2 we saw that the streamline diffusion form yields slightly better convergence than the first order accurate isotropic form $(h\nabla U, \nabla v)$; a scheme that switches from streamline to isotropic diffusion near shocks is studied e.g. in [26].

ETNA
Kent State University
etna@mcs.kent.edu

The Green's function X can be found by separation of variables; hypothesizing that $X(x_1, x_2, t) = \alpha(x_1, t)\beta(x_2, t)$, then (8.12) holds provided

$$\begin{aligned} \alpha_t + h_0[(u(x_1)\alpha)_{x_1} - h_0\alpha_{x_1x_1}] &= 0, \quad \alpha(\cdot\,, 0) = \delta(\cdot - \underline{x}_1), \\ \beta_t - h_0^2\beta_{x_2x_2} &= 0, \quad \beta(\cdot\,, 0) = \delta(\cdot - \underline{x}_2). \end{aligned}$$

We have

$$\beta(x_2, t) = \frac{1}{\sqrt{4\pi h_0^2 t}} \exp[-(x_2 - \underline{x}_2)^2/(4h_0^2 t)]. \tag{8.13a}$$

In fact, the function α also has an explicit solution, which can be derived by the Hopf-Cole transformation (see [15])

$$\alpha(x, t; \underline{x}_1, 0) = \int_{-\infty}^{\underline{x}_1} \varphi(y', 0; x, t)dy', \tag{8.13b}$$

where φ is the following sum of heat kernels

$$\begin{aligned} &\varphi(y, 0; x, t) \\ &= \tfrac{e^{-x/(2h_0)}}{e^{x/(2h_0)}+e^{-x/(2h_0)}}\partial_y H^+(x - y, t) + \tfrac{h_0^{-1}}{(e^{x/(2h_0)}+e^{-x/(2h_0)})^2}H^+(x - y, t) \\ &+ \tfrac{e^{x/(2h_0)}}{e^{x/(2h_0)}+e^{-x/(2h_0)}}\partial_y H^-(x - y, t) - \tfrac{h_0^{-1}}{(e^{x/(2h_0)}+e^{-x/(2h_0)})^2}H^-(x - y, t), \end{aligned} \tag{8.14a}$$

and

$$H^{\pm}(z, s) = H(z \mp s, s) = \frac{1}{\sqrt{4\pi h_0^2 s}} \exp\left[-(z \mp h_0 s)^2/(4h_0^2 s)\right]. \tag{8.14b}$$

In particular, since $(\frac{-1}{2}\tanh\frac{x}{2h_0})_x$ is the eigenfunction corresponding to the zero eigenvalue of $\mathcal{L}$, we have

$$\begin{aligned} &\alpha(x, t; \underline{x}_1, 0) - (\tfrac{-1}{2}\tanh\tfrac{x}{2h_0})_x \\ &= \textstyle\int_{\mathbb{R}}(\alpha(x', 0) - (\tfrac{-1}{2}\tanh\tfrac{x'}{2h_0})_{x'})\alpha(x, t; x', 0)dx' \\ &= \textstyle\int_{\mathbb{R}}(\text{sign}(\underline{x}_1 - x') - \tfrac{-1}{2}\tanh\tfrac{x'}{2h_0})\varphi(x', 0; x, t)dx' \\ &\le Ch_0^{-1}\exp(-c(|x|/h_0 + t)), \end{aligned} \tag{8.15a}$$

which implies

$$\int_{\mathbb{R}}(\alpha(x, t) - \frac{-1}{2}\tanh\frac{x}{2h_0})dx = 0. \tag{8.15b}$$

Here $\text{sign}(x) \equiv 1$, if $x > 0$ and $\text{sign}(x) \equiv -1$ if $x \le 0$. Equality (8.15b) follows from the fact that the function ω, dual to φ, defined by

$$\frac{\partial}{\partial x}\omega(x, t; y, 0) = \varphi(y, 0; x, t),$$

satisfies

$$\omega_t + h_0[u(x_1)\omega_{x_1} - h_0\Delta\omega] = 0, \quad \omega(\cdot\,, 0) = \delta(\cdot - y),$$

ETNA
Kent State University
etna@mcs.kent.edu

and hence

$$\int_{\mathbb{R}} \varphi(y,0;x,t)dx = \omega(\infty,t;y,0) - \omega(-\infty,t;y,0) = 0.$$

Our construction yields

$$X(x,t;\underline{x},0) = g(x,t;\underline{x},0) = \alpha(x_1,t;\underline{x}_1,0)\beta(x_2,t;\underline{x}_2,0), \tag{8.16}$$

and therefore, by (8.6), the smoothing operator S has an explicit expression. To determine the iteration error ξ, we shall solve for ξ in the residual equation

$$\mathcal{L}\xi = X. \tag{8.17a}$$

In the constant coefficient case we could directly obtain the solution of the stationary problem by Fourier methods. Now, we shall compute the solution of the stationary problem (8.17a) by means of the corresponding time dependent problem,

$$\bar{\xi}_t + h_0\mathcal{L}\bar{\xi} = h_0 X(\cdot\,,\nu;\underline{x},0), \tag{8.17b}$$

for which we know the Green's function. Then we shall use that

$$\xi(\cdot\,,\nu) = \lim_{t\to\infty} \bar{\xi}(\cdot\,,t).$$

When applying Duhamel's principle to the time dependent problem (8.17b), the space-time integrals will only be well defined provided the stationary solution is sufficiently localized, which for Green's functions depends on the number of space dimensions. In order to achieve sufficient locality, it is suitable to seek first $\bar{\xi}_{x_2x_2}$, which satisfies

$$\frac{\partial}{\partial t}\bar{\xi}_{x_2x_2} + h_0\mathcal{L}\bar{\xi}_{x_2x_2} = h_0 X_{x_2x_2}(\cdot\,,\nu;\mathrm{x},0),$$

since $\mathcal{L}$ is x_2 independent. Using that X is the Green's function of (8.12) and that α satisfies (8.15) we have

$$\begin{aligned} h_0\tfrac{\partial^2}{\partial x_2^2}\xi(x,\nu;\underline{x},0) &= \int_{\mathbb{R}^2}\int_0^\infty h_0^2\frac{\partial^2}{\partial x_2^2}X(x,t;y,0)X(y,\nu;\underline{x},0)dtdy \\ &= \tfrac{1}{\sqrt{4\pi\nu h_0^2}}\exp[-x_2^2/(4h_0^2\nu)](\tfrac{-1}{2}\tanh\tfrac{x_1}{2h_0})_{x_1} \\ &+ \int_{\mathbb{R}^2}\int_0^\infty(\alpha(x_1,t;y_1,0)-\alpha(x_1,\infty;y_1,0))\frac{h_0^2\partial^2}{\partial x_2^2}\beta(x_2,t;y_2,0)X(y,\nu;\underline{x},0)dtdy, \end{aligned} \tag{8.17c}$$

where the last term is localized and has zero mass due to (8.15). Therefore, by integrating the equation

$$(u\xi)_{x_1} - h_0\xi_{x_1x_1} = X - h_0\xi_{x_2x_2}$$

in the x_1-direction, we see that

$$\begin{aligned} \xi(x,\nu;\underline{x},0) &= \tfrac{1}{u(x_1)}\int_0^{x_1}(X(x',\nu;\underline{x},0) - h_0\xi(x,\nu;\mathrm{x},0)_{x_2x_2})dx_1' \\ &- \int_0^{x_1}(\frac{X(x',\nu;\underline{x},0) - h_0\xi(x',\nu;\underline{x},0)_{x_2x_2}}{u(x_1')})_{x_1'}\exp(A(x_1')-A(x_1))dx_1' \end{aligned} \tag{8.18}$$

ETNA
Kent State University
etna@mcs.kent.edu

is a solution. Here $\frac{d}{dy}A(y) = u(y)$. The equations (8.18) and (8.2) show that the residual parts $(u\xi)_{x_1}$, $h_1\xi_{x_1x_1}$ and $h_1\xi_{x_2x_2}$ in (8.11) are localized functions bounded by

$$C\frac{1}{\sqrt{4\pi\nu h_0^2}}\exp[-x_2^2/(ch_0^2\nu)](\frac{-1}{2}\tanh\frac{cx_1}{2h_0})_{x_1},$$

where C and c are positive constants. By replacing h_0 with h_1 in (8.17-18) we obtain the same estimates for $P_1\xi$ as for ξ, where

$$(uP_1\xi)_{x_1} - h_1\Delta P_1\xi = X. \tag{8.19}$$

Using that $K^* = K$, we then note that the projection part of the residual error satisfies

$$|SK(u\xi)_{x_1}| = \left|\int_{\boldsymbol{R}^2} K_y X(x,\nu;y,0)(u(y_1)\xi(y,\nu;\underline{x},0))_{y_1}dy\right| \leq \frac{C}{\nu}, \tag{8.20}$$

and similarly for the contributions from $h_0\Delta\xi$, $(uP_1\xi)_{x_1}$ and $h_1\Delta P_1\xi$. To obtain (8.20) we used the explicit expression (8.13), (8.16) of X. In (8.20) it is important to note that the y_1-derivatives in K, cf. (8.10), makes the Green's function X decay exponentially fast in t, (since by (8.13b) φ is localized around $x = \pm h_0 t$) for $\mathbf{x}$ in the shock region, while the y_2-derivatives in K yield parabolic damping. The exponential damping is also seen in (8.15a).

Using the decomposition (8.17), (8.6) and (8.15), (8.17), (8.20) we see that the L_1-norm of the error from the artificial diffusion

$$(h_0 - h_1)S(P_1\xi)_{x_2x_2} = \frac{-h_1}{2}S(P_1\xi)_{x_2x_2}$$

is bounded by $1/2 + C\exp(-c\nu)$. The terms $1/2$ and $\exp(-c\nu)$ correspond to the first and second term, respectively, of the right hand side in (8.17). The exponential bound follows by using (8.15b) and integrate by parts in the x_1-direction to get a factor $X(x,t;y,0)_{y_1} = \varphi\beta$. The L_1-norm of the remaining error $(h_0 - h_1)S(P_1\xi)_{x_1x_1}$ is bounded by $C\exp(-c\nu)$ using that ξ_{x_1} is a localized bounded mass and that $X(x,\nu;y,0)_{y_1}$ is decaying exponentially fast in time ν. By combining all estimates of the residual error in (8.11), we obtain

THEOREM 1.2. *Assume that the residual error $\mathcal{L}U_0$, for the continuous version of the two grid method applied to the shock wave problem (8.2), initially is localized in the shock wave region B, i.e. $\mathcal{L}U_0(x) = 0$ for $x \notin B = \{(x_1,x_2) \in \boldsymbol{R}^2 : |x_1| \leq Ch_0\}$. Then one iteration of the continuous two-grid cycle, with ν pre and post smoothing steps, damps the residual with a factor*

$$\gamma_B = \frac{\|\mathcal{L}U_{next}\|_{L_1(\boldsymbol{R}^2)}}{\|\mathcal{L}U_0\|_{L_1(\boldsymbol{R}^2)}} \leq \frac{1}{2} + \frac{C}{\nu}.$$

This indicates that a residual error, localized in the shock region, is damped by the two grid method, provided sufficiently many smoothing steps ν are used.

To convert this analysis to a rigorous convergence proof for the discrete version of the two-level method would require analogous estimates of the discrete version of the residual X. Theorem 1.1 shows that the derivation (3.16-24) make sense for problem (1.1), we therefore expect that the discussion above also is relevant in the fully discrete case.

8.3. Numerical test. In Fig. 5 we present numerical results of the two grid method applied to the nonlinear shock wave problem (8.1) confirming the 1/2 in Theorem 1.2. Fig. 6 shows the result of using an adaptive space-time finite element method for a time dependent Burgers problem, using the nonlinear full multigrid method; see [14], [25].

ETNA
Kent State University
etna@mcs.kent.edu

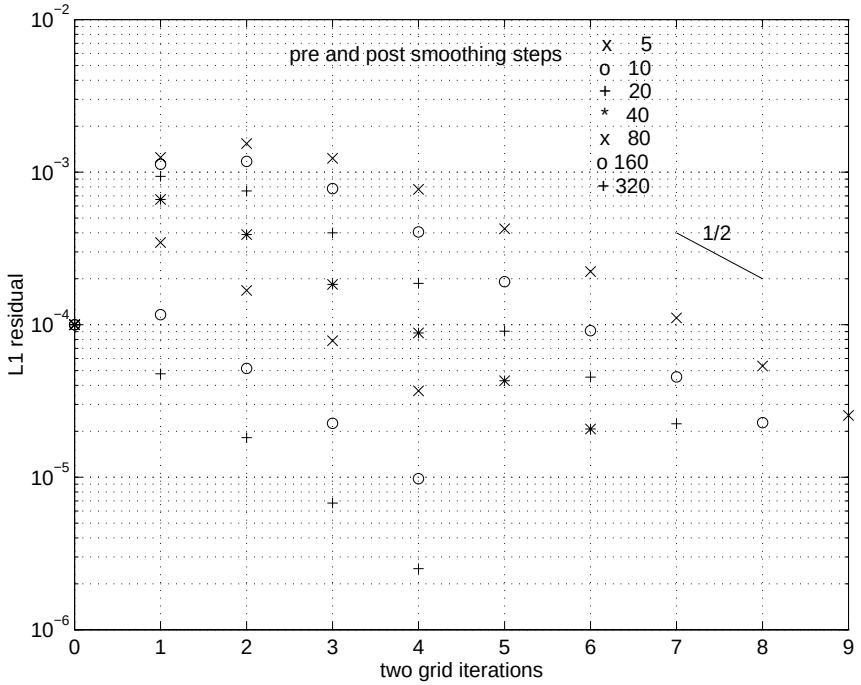

FIG. 5. *Convergence of the two grid method for a nonmoving Burgers shock. The computational domain is* $(0,1) \times (0,1)$ *with Dirichlet boundary conditions* $u(x_1, x_2) = u_0(x_1) = -\tanh(x_1 - 0.5/2/0.01)$. *The equation is solved on the uniform grids with fine grid* $h_0 = 1/32$ *and coarse grid* $h_1 = 1/16$ *with isotropic artificial diffusion* $h_j \Delta u$, *j=0,1. We use Jacobi smoothing steps with damping constant* $c = 0.2$, *and* $\nu_{pre} = \nu_{post}$. *The finite-dimensional equation has been solved accurately when a small Dirac-like residual with* L_1*-norm* 10^{-4} *is introduced by addition to the right hand side of the assembled equation. In the figure the* L_1*-norm of the residual with different number of smoothing steps are plotted. Note that the convergence after an increase settles down to a damping factor 1/2. The mass,* $\int_{(0,1)\times(0,1)} R dx$, *of the residual* R *is damped by the factor* $1/2$ *as given by theory, This is a difficult problem to solve when only using Jacobi smoothing. Experiments show that it takes asymptotically 1440 Jacobi iterations to damp the* L_1*-norm of the residual by a factor* $1/2$. *In the figure this finite dimensional effect starts to influence the convergence rate when the number of smoothing steps are 160 and 320.*

ETNA
Kent State University
etna@mcs.kent.edu

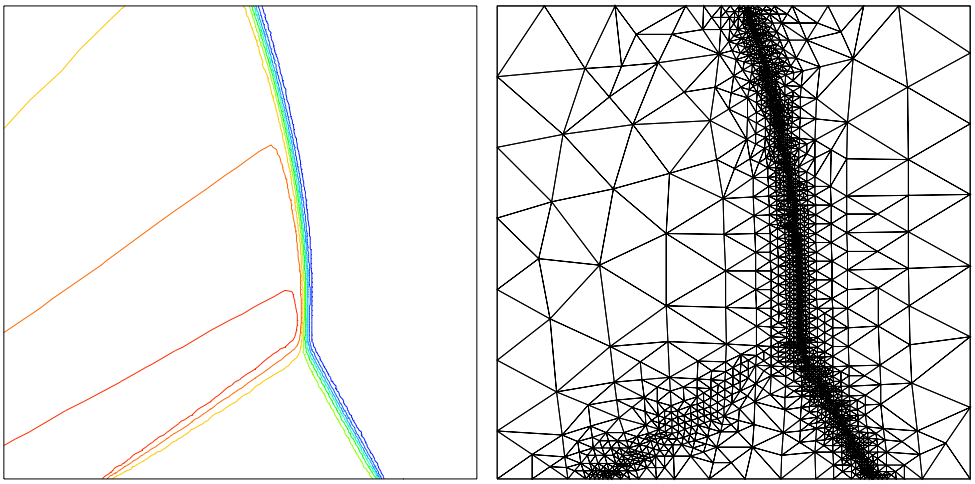

FIG. 6. *Two colliding Burgers shocks solving* $u_t + uu_x = \epsilon u_{xx}$, $u(x,0) = u_0(x)$, *with* $\epsilon = 0.01$ *in the space-time domain. The approximate problem is solved with piecewise quadratic elements using streamline diffusion stabilization and the nonlinear multigrid method. The correction problems use piecewise linear elements with isotropic artificial diffusion; see [14], [25]. The figures show the adapted grid and the solution after 5 refinements. The initial data* u_0 *is piecewise linear and the analytical solution is computed by the Hopf-Cole transform. The solution in the figure has a relative* L_∞*-error of 2.5%. The mesh contains 3730 triangles and has 7432 degrees of freedom.*

9. Boundary conditions. In an unbounded domain, the L_1-norm damping γ_∞ of the multigrid method in (1.10) becomes unbounded due to the factor $\log(B/h_j)$. Therefore, for a convection dominated problem to prove that a V-cycle forms an L_1-contraction for the residual, we need to study bounded domains and boundary effects. Our method to analyze the damping is based on Green's functions. Hence, we would like to know Green's functions for (1.1) including boundary conditions. We study here the following variant of boundary conditions for (1.1)

$$\begin{aligned} L_0 U \equiv u(x_1) U_{x_1} - \epsilon \Delta U &= f, \quad x_1 < 0, \\ U(0, x_2, t) &= 0, \end{aligned} \tag{9.1}$$

where $u(x_1) = -\tanh(x_1/(2\epsilon))$ is the solution of Burgers equation (8.1). We can view (9.1) as a kind of Dirichlet boundary condition at $x_1 = 0$ for (1.1), with a small modification of the flow $(1,0)$ near the boundary. For the problem (9.1), we now construct Green's functions by means of the dual solutions φ and β in (8.13) and (8.14). Then, following Section 8, we use the Green's function to study L_1-convergence for the continuous version of the two grid method. We have

THEOREM 9.1. *Assume that there are positive constants* B, C *such that the initial residual,* $L_0 U_0 - f$*, satisfies*

$$\int_{-\infty}^{x_1} \int_{\boldsymbol{R}} |(L_0 U_0 - f)((x_1', x_2))| dx_1' dx_2 \leq \|L_0 U_0 - f\|_{L_1((-\infty,0)\times \boldsymbol{R})} \exp[(x_1 + B)/C],$$

ETNA
Kent State University
etna@mcs.kent.edu

for $x_1 \leq -B$. Then one iteration of the continuous two-grid cycle, with ν_0 pre and post smoothing steps, damps the residual with a factor

$$\frac{\|L_0 U_{next} - f\|_{L_1((-\infty,0)\times \boldsymbol{R})}}{\|L_0 U_0 - f\|_{L_1((-\infty,0)\times \boldsymbol{R})}} \leq \left[\frac{C_1 h_0 \log(B/h_0)}{\epsilon \nu_0} + \frac{C_2}{\sqrt{\nu}_0}\right](1 + \frac{C_0 h_0}{\epsilon \nu_0}).$$

Furthermore, the residual of the next iteration satisfies the same localized estimate as the initial residual

$$\int_{-\infty}^{x_1}\int_{\boldsymbol{R}} |(L_0 U_{next} - f)(x_1', x_2))| dx_1' dx_2 \leq \|L_0 U_{next} - f\|_{L_1(-\infty,0)\times \boldsymbol{R})} \exp[(x_1 + B)/C],$$

for $x_1 \leq -B$, and there is a positive constant C' such that the continuous version of the two-grid method is a contraction for the residual in $L_1((-\infty, 0) \times \boldsymbol{R})$, provided

$$\nu_0 \geq C' + \frac{C' h_0 \log(B/h_0)}{\epsilon}.$$

Proof. The following sum of convected heat kernels $H^{\pm}$, given in (8.14),

$$\begin{aligned}
&\psi(y,t;x,s;h_0) \equiv \int_{-\infty}^{x} \varphi(y,t;x',s;h_0)dx' \\
&= \tfrac{e^{-x/(2h_0)}}{e^{x/(2h_0)}+e^{-x/(2h_0)}} H^+(x-y,s-t) + \tfrac{e^{x/(2h_0)}}{e^{x/(2h_0)}+e^{-x/(2h_0)}} H^-(x-y,s-t),
\end{aligned}$$

solves

$$\begin{aligned}
-\psi_t - h_0[(u(x_1)\psi)_{x_1} - h_0\psi_{x_1x_1}] &= 0, \\
\psi(y,\bar{t};x,\bar{t}) &= \delta(x-y).
\end{aligned}$$

Let

$$\beta(y_2,t;x_2,\bar{t}) = \frac{1}{\sqrt{4\pi\epsilon h_0(\bar{t}-t)}} \exp[-(x_2-y_2)^2/(4\epsilon h_0(\bar{t}-t))],$$

and define

$$\widetilde{\psi}(y,t;x,\bar{t};h_0) \equiv \psi(y_1,t;x_1,\bar{t};h_0)\beta(y_2,t;x_2,\bar{t}),$$

which satisfies the backward problem

$$\begin{aligned}
-\widetilde{\psi}_t - h_0[(u(x_1)\widetilde{\psi})_{x_1} - h_0\widetilde{\psi}_{x_1x_1} - \epsilon\widetilde{\psi}_{x_2x_2}] &= 0, \ \ t < \bar{t}, \\
\widetilde{\psi}(y,\bar{t};x,\bar{t}) &= \delta(x-y).
\end{aligned}$$

Thus, the function $\widetilde{\psi}(y,0;x,t)$ is the Green's function of the forward problem

$$\begin{aligned}
\widehat{\xi}_t + h_0 L_0 \widehat{\xi} \equiv \widehat{\xi}_t + h_0[(u(x_1)\widehat{\xi})_{x_1} - h_0\widehat{\xi}_{x_1x_1} - \epsilon\widehat{\xi}_{x_2x_2}] &= 0, \quad x \in \boldsymbol{R}^2, \ \ t > 0, \\
\widehat{\xi}(x,0) &= \widehat{\xi}_0.
\end{aligned} \tag{9.2}$$

Now let the initial iteration error $\widehat{\xi}(\cdot\,,t)$, for some $y = (y_1, y_2) \in (-\infty, 0) \times \boldsymbol{R}$, satisfy

$$\begin{aligned}
L_0\widehat{\xi}(x,0;y,0) &= \delta(x-y), \ \ x = (x_1,x_2) \in (-\infty,0)\times\boldsymbol{R}, \\
\widehat{\xi}(0,0;y,0) &= 0.
\end{aligned}$$

ETNA
Kent State University
etna@mcs.kent.edu

Then, we extend, for fixed x_2 and y, the iteration error $\widehat{\xi}((\cdot\,, x_2), 0; y, 0)$ to an odd function in $\boldsymbol{R}$, and conclude that $\widehat{\xi}$ satisfies (9.2) with the condition $\widehat{\xi}((0, x_2), t; y, 0) = 0$. Furthermore, the definition $X \equiv L_0\widehat{\xi}$ and the fact $\partial_t L_0 = 0$ imply

$$\begin{aligned} X_t + h_0 L_0 X &= 0, \quad x \in \boldsymbol{R}^2, \\ X(x,0) &= \delta(x-y) - \delta(x+y). \end{aligned} \tag{9.3}$$

Using that $\widetilde{\psi}$ is dual to X and $\widehat{\xi}$, we obtain as in (8.16)

$$X(x,\nu) = \widetilde{\psi}(y,0;x,\nu;h_0) - \widetilde{\psi}(-y,0;x,\nu;h_0),$$

and by solving the equation $L_0\widehat{\xi} = X$, by means of the time dependent problem as in (8.17), yields

$$\begin{aligned} \widehat{\xi}(x,\nu;y,0) &= \textstyle\int_0^\infty \int_{\boldsymbol{R}^2} \widetilde{\psi}(y',0;x,t;h_0) X(y',\nu)\,dy'dt \\ &= \textstyle\int_0^\infty \int_{\boldsymbol{R}^2} \widetilde{\psi}(y',0;x,t;h_0)[\widetilde{\psi}(y,0;y',\nu;h_0) - \widetilde{\psi}(-y,0;y',\nu;h_0)]\,dy'dt. \end{aligned} \tag{9.4}$$

Hence we have an explicit expression for $\widehat{\xi}$, and therefore, the residual error (8.11) for the continuous version of the two grid method can be evaluated.

The corresponding solution ξ in (3.16), without boundary condition at $x_1 = 0$, satisfies

$$\xi(x,\nu;y,0) = \int_0^\infty \int_{\boldsymbol{R}^2} \lim_{h\to 0+} \widetilde{\psi}(y,0;x,t;h)\widetilde{\psi}(y,0;y',\nu;h)\,dy'dt, \tag{9.5}$$

and is estimated in (3.20) and Lemma 5.1. The right hand side in (9.4) has two terms of the same type as in (9.5), and it can be shown, using Lemma 8.1 and (8.11), that the residual error for the continuous two grid method based on $\widehat{\xi}$ has the same damping γ_B as ξ in (1.9) and (1.10).

To study L_1-convergence of the continuous two grid method we also need that the residual decays sufficiently fast for $x_1 \to -\infty$. Let us now assume that the initial residual error $L_0U_0 = R$ satisfies

$$\int_{-\infty}^{x_1} \int_{\boldsymbol{R}} |R((x_1', x_2))|\,dx_1'\,dx_2 \le \|R\|_{L_1} \exp[(x_1+B)/C] \ \text{ for } x_1 \le -B. \tag{9.6}$$

The representation (9.4) and analogues of (3.20), (5.7), (5.8d) imply

$$\int_{\boldsymbol{R}} (|\widehat{\xi}(x,t;y,0)_{x_1}| + h_0|\widehat{\xi}_{x_1x_1}| + \epsilon|\widehat{\xi}_{x_2x_2}|)\,dy_2 \le \begin{cases} \frac{C}{x_1-y_1} + \frac{Ch_0}{(x_1-y_1)^2}, & \text{for } x_1 - y_1 \ge h_0\sqrt{\nu}, \\ C\exp[\frac{y_1-x_1}{ch_0}], & \text{for } x_1 - y_1 < h_0\sqrt{\nu}. \end{cases}$$

Then, using also (9.4), (1.10) and $U_0(x) = \int_{\boldsymbol{R}^2} R(y)\widehat{\xi}(x,0;y,0)\,dy$, we see by the residual representation (8.11) that the next iteration yields a residual which satisfies the decay in (9.6)

$$\int_{-\infty}^{x_1} \int_{\boldsymbol{R}} |L_0 U_{\text{next}}|\,dx_2\,dx_1 \le \|R\|_{L_1} \exp[(x_1+B)/C] \quad \text{for } x_1 \le -B,$$

and the damping

$$\frac{\|L_0 U_{\text{next}}\|_{L_1}}{\|L_0U_0\|_{L_1}} \le \gamma_B,$$

ETNA
Kent State University
etna@mcs.kent.edu

where γ_B satisfies the bound in (1.10). Therefore, the continuous version of the two grid method with the boundary condition (9.1) and the initial decay (9.6) gives a contraction for the residual in L_1, provided sufficiently many smoothing steps are used. □

The corresponding case of a Neumann boundary condition at $x_1 = 0$ can be studied similarly by replacing odd by even and the $-\delta,\ -\widetilde{\psi}$ in (9.3) and (9.4) by $+\delta,\ +\widetilde{\psi}$, respectively.

REFERENCES

[1] R. E. BANK, *A comparison of two multi-level iterative methods for nonsymmetric and indefinite elliptic finite element equations*, SIAM J. Numer. Anal., 18 (1981), pp. 724–743.
[2] R. E. BANK AND M. BENBOURENANE, *The hierarchical basis multigrid method for convection- diffusion equations*, Numer. Math., 61 (1992), pp. 7–37.
[3] R. E. BANK AND T. DUPONT, *An optimal order process for solving finite element equations*, Math. Comp., 36 (1981), pp. 35–51.
[4] R. BECKER, C. JOHNSON AND R. RANNACHER, *Adaptive error control for multigrid finite element methods*, Computing 55 (1995), no. 4, 271–288.
[5] J. H. BRAMBLE, *Multigrid Methods*, Pitman research notes in mathematical sciences, 1993.
[6] J. H. BRAMBLE, D. Y. KWAK AND J. E. PASCIAK, *Uniform convergence of multigrid V-cycle iterations for indefinite and nonsymmetric problems*, SIAM J. Numer. Anal., 31 (1994), pp. 1746–1763.
[7] A. BRANDT, *Multi-level adaptive solutions of boundary-value problems*, Math. Comp., 31 (1977), pp. 333–390.
[8] A. BRANDT, *Multigrid Techniques*: *1984 Guide with Applications to Fluid Dynamics*, GMD-Studien Nr. 85, 1984.
[9] A. BRANDT AND I. YAVNEH, *On multigrid solution of high-Reynolds incompressible flows*, J. Comput. Phys., 101 (1992), pp. 151–164.
[10] S. BRENNER AND R. SCOTT, *The Mathematical Theory of Finite Element Methods*, Springer-Verlag, 1994.
[11] X. -C. CAI AND M. SARKUS, *Local multiplicative Schwarz algorithms for steady and unsteady convection-diffusion equations*, East-West J. Numer. Math. 6 (1998), no. 1, 27–41.
[12] T. CHAN AND T. MATHEW, *Domain decomposition methods*, Acta Numerica, 1992.
[13] J. DOUGLAS, T. DUPONT AND L. WAHLBIN, *The stability in L^q of the L^2-projection into finite element function spaces*, Numer. Math., 23 (1975), pp. 193-197.
[14] J. GOODMAN, K. SAMUELSSON AND A. SZEPESSY, *Anisotropic refinement algorithms for finite elements*, Report NADA, KTH, Stockholm.
[15] J. GOODMAN, A. SZEPESSY AND K. ZUMBRUN, *A remark on the stability of viscous shock waves*, SIAM J. Math. Anal., 25 (1994), pp. 1463–1467.
[16] W. HACKBUSH, *Multigrid convergence for a singular perturbed problem*, Linear Algebra Appl., 58 (1984), pp. 125–145.
[17] W. HACKBUSH, *Multigrid Methods and Applications*, Springer-Verlag, 1985.
[18] A. JAMESON, *Computational transonics*, Comm. Pure Appl. Math., XLI (1988), pp. 507–549.
[19] C. JOHNSON, U. NÄVERT AND J. PITKÄRANTA, *Finite element methods for linear hyperbolic problems*, Comput. Methods Appl. Mech. Engng., 45 (1984), pp. 329-336.
[20] C. JOHNSON AND A. SZEPESSY, *Adaptive finite element methods for conservation laws based on a posteriori error estimates*, Comm. Pure Appl. Math., 98 (1995), pp. 199–234.
[21] H. KREISS AND J. LORENTZ, *Initial-Boundary Value Problems and the Navier-Stokes Equations*, Academic Press, 1989.
[22] P. LÖTSTEDT AND B. GUSTAFSSON, *Fourier analysis of multigrid methods for general systems of PDEs*, Math. Comp., 60 (1993), pp. 473–493.
[23] T.P. MATHEW, *Uniform convergence of the Schwarz alternating method for solving singularly perturbed advection-diffusion equations*, preprint, 1995.
[24] A. REUSKEN, *Fourier analysis of a robust multigrid method for convection-diffusion equations*, Numer. Math., 71 (1995), no. 3, 365–397.
[25] K. SAMUELSSON, *Adaptive Algorithms for Finite Element Methods Approximating Flow Problems*, Doctoral Thesis, NADA, KTH, Stockholm, 1996.
[26] A. SZEPESSY, *Convergence of a shock-capturing streamline diffusion finite element method for a scalar conservation law in two space dimensions*, Math. Comp., 53 (1989), pp. 527–545.